

Title A neurocomputational theory of action regulation predicts motor behavior in neurotypical individuals and patients with Parkinson's disease

S. Zhong¹, J. Choi², N. Hashoush³, D. Babayan³, M. Malekmohammadi³, N. Pouratian^{2,¶}, V. N. Christopoulos^{1,4,¶}

¹Neuroscience graduate program, University of California Riverside, Riverside, CA, USA

²Department of Neurological Surgery, UT Southwestern Medical Center, Dallas, TX, USA

³David Geffen Sch. of Med., University of California Los Angeles, Los Angeles, CA

⁴Department of Bioengineering, University of California Riverside, Riverside, CA, USA

¶ These authors jointly supervised this work (Correspondence)

* E-mail: Corresponding vchristo@engr.ucr.edu , Nader.pouratian@utsouthwestern.edu

Abstract

Surviving in an uncertain environment requires not only the ability to select the best action, but also the flexibility to withhold inappropriate actions when the environmental conditions change. Although selecting and withholding actions have been extensively studied in both human and animals, there is still lack of consensus on the mechanism underlying these action regulation functions, and more importantly, how they inter-relate. A critical gap impeding progress is the lack of a computational theory that will integrate the mechanisms of action regulation into a unified framework. The current study aims to advance our understanding by developing a neurodynamical computational theory that models the mechanism of action regulation that involves suppressing responses, and predicts how disruption of this mechanism can lead to motor deficits in Parkinson's disease

(PD) patients. We tested the model predictions in neurotypical individuals and PD patients in three behavioral tasks that involve free action selection between two opposed directions, action selection in the presence of conflicting information and abandoning an ongoing action when a stop signal is presented. Our results and theory suggest an integrated mechanism of action regulation that affects both action initiation and inhibition. When this mechanism is disrupted, motor behavior is affected, leading to longer reaction times and higher error rates in action inhibition.

Author Summary

Humans can rapidly regulate actions according to updated demands of the environment. A key component of action regulation is action inhibition, the failure of which contributes to various neuropsychiatric disorders. When faced with multiple choices, dealing with conflicting information, or current actions become inappropriate or unwanted, we should be able to pause or completely abandon actions. Despite extensive efforts to understand how the brain selects, pauses, and abandons actions based on environmental demands, the mechanisms underlying these action regulation functions and, perhaps more importantly, how they inter-relate remain elusive. Part of this challenge lies in the fact that these mechanisms were rarely explored together, making it difficult to develop a unified theory that explains the computational aspects of action regulation functions. The current study introduces a large-scale model that better characterizes the computations of action regulation functions, how they are implemented within brain networks that involve frontal, motor and basal ganglia (BG) circuits, and how disruption of these circuits can lead to deficits in motor behavior seen in Parkinson's disease (PD). The model was developed by studying the motor behavior of healthy individuals and PD patients in three motor tasks

that involve action inhibition. Overall, the model explains many key aspects on how the brain regulates actions that involve inhibitory processes, opening new avenues for improving and developing therapeutic interventions for diseases that may involve these circuits.

1 Introduction

Surviving in an uncertain environment requires not only the ability to accurately and rapidly select the best action, but also the flexibility to abandon obsolete actions when they are rendered unwanted or inappropriate. How actions are initiated and regulated is a fundamental neurobiological question that is of high impact for understanding how the human brain functions. A key component of action regulation is inhibiting actions, which when abnormal contributes to neuropsychiatric diseases, such as Parkinson's disease (PD), obsessive-compulsive disorder (OCD), and others [1–5]. Action inhibition occurs in at least 3 ways: (a) action selection – selecting one action requires suppressing alternative motor plans, (b) decision conflict – choosing in the presence of conflicting information requires suppressing alternative actions to buy more time to make a correct decision and (c) outright stopping – inhibiting a response when it is rendered inappropriate.

Over the past years, a number of studies attempted to characterize the mechanism of action regulation that involves action inhibition under different experimental paradigms. A recent cognitive theory suggests that action selection occurs through a competitive process between movement plans [6–10]. According to this theory, in situations affording more than one alternatives, animals prepare multiple actions in parallel that compete for selection through mutual inhibitory interactions before choosing to execute one. This affordance competition theory received empirical support from neurophysiological inves-

70 tifications in the sensorimotor areas of non-human primates (NHPs) showing that the
71 brain encodes parallel reach, grasp and saccade plans before the animals select between
72 them [11–13]. It is consistent with the continuous flow model of perception, which sug-
73 gests that response preparation can begin even before the goal is fully identified and a
74 decision is made [14–16]. In addition, psychophysical support for this theory comes from
75 the “go-before-you-know” experiments, in which individuals had to initiate reaching or
76 saccade movements towards multiple potential targets, without knowing the actual lo-
77 cation of the goal [17–19]. The individuals compensate for the goal location uncertainty
78 by aiming towards an intermediate location, a strategy consistent with an averaging of
79 multiple competing action plans.

80 Recent studies have also explored the mechanisms underlying pausing or abandon-
81 ing actions using functional MRI [20, 21], local field potential (LFP) recordings [22, 23],
82 electroencephalography (EEG) recordings [24, 25], as well as single-unit recordings in hu-
83 mans [26, 27], non-human primates (NHPs) [28, 29] and rodents [30]. The basal ganglia
84 (BG), and in particular the subthalamic nucleus (STN), has been functionally implicated
85 in action regulation functions, but in association with distinct frontal areas, such as the
86 primary motor cortex (M1), the premotor cortex (preMC), the pre-supplementary motor
87 area (preSMA) and the right inferior frontal gyrus (rIFG) [31–34]. In a sense, STN is acti-
88 vated when a stop signal is detected, as well as when conflicting information is presented,
89 to rapidly suppress ongoing or planned actions [35–37].

90 Despite the significant contribution of these studies on understanding how the brain
91 selects between competing options, deals with conflicting information, and stops planned
92 or ongoing actions during decisions, the mechanisms of these action regulation functions
93 and their inter-relations remain elusive. Part of this challenge lies in the fact that previ-
94 ous studies rarely explore these functions together, making it difficult to develop a unified

95 and integrated theory of action regulation. The current study aims to advance our un-
 96 derstanding on the mechanism underlying action regulation and how disruption of this
 97 mechanism can lead to deficits in motor behavior exhibited in Parkinson's disease (PD).
 98 To address these questions, we trained neurotypical individuals and PD patients to per-
 99 form three motor tasks that involve motor decision between two opposed directions, action
 100 selection in the presence of conflicting information and suppression of unwanted motor re-
 101 sponses when a stop signal is presented. To elucidate the action regulation mechanism in
 102 control and disease state, we modeled the tasks within a neurodynamical computational
 103 framework that combines dynamic field theory with stochastic optimal control theory,
 104 and simulates the processes underlying selection, planning, initiation and suppression of
 105 actions [38, 39].

106 Our study presents the first unified theory on action regulation that involves response
 107 inhibition, providing important predictions on how the disruption of major nodes, such
 108 as STN, can deteriorate motor performance leading to longer reaction times in motor
 109 decisions and higher error rates when stopping ongoing actions. Additionally, the neu-
 110 rodynamical theory provides a potential explanation on why PD patients exhibit longer
 111 reaction times than neurotypical individuals even in the lack of competing alternatives
 112 or conflicting information in motor decisions. Overall, our findings shed light on how
 113 the brain regulates actions that involve inhibitory processes, opening new avenues for
 114 improving and developing therapeutic interventions for diseases that may involve these
 115 circuits.

116 2 Results

117 2.1 Experimental paradigms

118 Participants were instructed to perform reaching movements using a 2-dimensional joy-
 119 stick under three experimental paradigms: i) decision-making task (action selection), ii)
 120 Eriksen flanker task (decision conflict) and iii) stop-signal task (outright stopping) (Fig.1).
 121 In the decision-making task, participants had to respond to arrow stimuli presented on a
 122 computer screen by freely moving the joystick towards the left or right direction. Choice
 123 trials were interleaved with instructed trials in which all arrows pointed to the same di-
 124 rection. In the Eriksen flanker task, flanking arrows were presented on the screen, all
 125 pointing to the same direction. A target arrow was then presented to indicate the di-
 126 rection to move, either in the same (no conflict, congruent trials) or opposite (conflict,
 127 incongruent trials) direction as the flanking arrows. Finally, in the stop-signal task, the
 128 participants were instructed to reach towards the direction of the arrows. In a minority
 129 of trials, the color of the arrows turned red after a short delay, and the action had to be
 130 abandoned immediately.

131 _____

132 Figure 1 somewhere here

133 _____

134 2.2 Motor behavior of neurotypical individuals and PD patients 135 in action regulation tasks

136 We computed the reaction time (RT) for initiating an action as the time interval between
 137 the presentation of the target arrows on the screen and the initiation of the reaching

138 movement. We found that in the decision-making task, choice trials had longer RT than
 139 instructed trials in both populations (Fig. 2A) ($p < 0.001$, two-way ANOVA). Interest-
 140 ingly, although the neurotypical participants responded faster than the PD patients in
 141 the instructed trials ($p < 0.001$, two-way ANOVA), we found no significant difference in
 142 RT between the two groups in the choice trials ($p = 0.878$, two-way ANOVA), (Fig.2A). In
 143 the Eriksen flanker task, both groups exhibited shorter RT in the congruent trials than
 144 in the incongruent trials (Fig. 2B) ($p < 0.001$ for both neurotypical participants and PD
 145 patients, two-way ANOVA). However, PD patients had slower responses than neurotypical
 146 participants in both congruent and incongruent trials ($p < 0.01$ for congruent trials, $p < 0.05$
 147 for incongruent trials, two-way ANOVA). Regarding the stop-signal task, interestingly,
 148 we found that neurotypical participants had slower responses than PD patients in the go
 149 trials (Fig.2C) ($p < 0.001$, two sample t-test). In particular, the neurotypical group seems
 150 to have strategically slowed down their responses in the go trials by 233 ms on average
 151 in order to be more successful in inhibiting their response in stop trials ($p < 0.001$, two
 152 sample t-test on RT between instructed trials and go trials for the neurotypical popu-
 153 lation). On the other hand, PD patients exhibited much subtler modification of their
 154 response between instructed trials (decision-making task) and go trials (stop-signal task)
 155 - the reaction time for go trials increased only by 47 ms on average compared to instructed
 156 trials ($p < 0.001$, two sample t-test), suggesting that the anticipation of the stop signal had
 157 smaller effect on their motor planning behavior.

158

159

Figure 2 somewhere here

160

161

162

These findings predict that PD patients will perform worse in stop trials than neurotypical participants, since a lower probability of stopping has often been associated with

163 faster responses in go trials [40–42]. To test this hypothesis, we computed the probability
164 to stop an action for different stop-signal delay (SSD) values across all participants in
165 each group. The results showed that the probability to successfully stop an action was
166 inversely correlated with SSD, and consistent with the hypothesis, PD patients exhibited
167 lower probability of stopping an action compared to neurotypical individuals (Fig.3).

168

169

Figure 3 somewhere here

170

171 **2.3 An integrated neurodynamical theory of action regulation** 172 **predicts motor behavior**

173 Our findings require a computational theory that could explain the mechanism of action
174 regulation that involves inhibition and predicts how disruption of this mechanism can
175 lead to motor impairments in PD patients. Building on our previous successful work in
176 modeling visuomotor tasks [38, 39], we developed a neurodynamical theory to unify the
177 action regulation mechanism that involves inhibition. The theory builds on the affordance
178 competition hypothesis, according to which multiple actions are formed concurrently and
179 compete over time until one has sufficient evidence to win the competition [6, 7, 12].
180 It combines dynamic neural field (DNF) theory [43, 44] with stochastic optimal control
181 theory [45, 46] and its architectural organization is illustrated in Fig.4. Each DNF field
182 simulates the dynamic evolution of firing rate activity of a network of neurons over a
183 continuous space with local excitation and surround inhibition. It consists of 181 neurons
184 - with exception of the context signal field and the pause field - and each of them has
185 a preferred direction between 0° and 180°. The “spatial sensory input” field encodes

the angular representation of the competing actions (i.e., left vs. right movements in our study). The “expected outcome” field encodes the expected reward for reaching to a particular direction. The outputs of these two fields send excitatory projections (green arrows) to the “reach planning” field in a topological manner. The “reach cost” field encodes the effort cost required to implement an action at a given time and state. The reach cost field sends inhibitory projections (red arrow) to the reach planning field to penalize high-effort actions. For instance, an action that requires changing of moving direction is more “costly” than an action of keeping going in the same direction. Although the cost field does not have a critical role in this study, since all planning actions are associated with about same effort, it is required for generating reaching movements from the optimal control part of the model.

We also added to the model architecture a Basal Ganglia (BG)-type mechanism for implementing the inhibitory process. This mechanism consists of three DNF platforms: (a) two context signal fields (stop and conflict) that represent information related to the contextual requirement of the tasks; (b) a pause field that suppresses the activity of the reach planning field to inhibit planned or ongoing actions. Each of the context fields consist of 100 neurons which project to the corresponding sub-population of the pause field via one-to-all excitatory connections. The stop signal field and the conflict signal field are activated when they detect a stop cue and conflict cue, respectively. Regarding the action selection function, the model does not need a context field to signal the decision task, since it can collect this information from the spatial sensory input field. In particular, the spatial sensory input field projects to the corresponding sub-population on the pause field with one-to-all excitatory connections. If more than one targets is encoded in the spatial sensory input field, the corresponding population on the pause field is triggered. Notably, this architecture is consistent with experimental studies which suggest dissociable frontal-

211 BG circuits for different action suppression functions [34]. The pause field consists of 3
 212 sub-populations of 75 neurons, each of them associated with one of the action regulation
 213 functions (i.e., action decisions between multiple options, action selection in the presence
 214 of conflicting information and outright stopping of actions). Once the pause field is
 215 triggered, the activity of the reach planning field is suppressed to delay a decision when
 216 more time is needed (i.e. during action selection or decision with conflicting information),
 217 or to completely suppress an action when it is no longer wanted or rendered inappropriate
 218 (i.e., outright stopping).

219 Each neuron in the reach planning field is connected with a stochastic optimal con-
 220 troller. Once the activity of a reach neuron j exceeds the action initiation threshold (cyan
 221 discontinuous line in Fig.4) at the current time and state \mathbf{x}_t , the corresponding controller
 222 initiates an optimal policy $\pi_j(\mathbf{x}_t)$ to move the joystick towards the preferred direction of
 223 that neuron (see materials and methods section for more details). Reaching movements
 224 are generated as a mixture of active policies (i.e., policies in which the associated neuronal
 225 activity in the reach planning field is above the action initiation threshold) weighted by
 226 the normalized activity of the corresponding reaching neurons. The normalized activity
 227 is called relative desirability since it reflects the *attractiveness* of a policy with respect to
 228 alternatives (for more details see [19, 38]).

229

230 Figure 4 somewhere here

231

232 2.3.1 Modeling the computations of motor decision-making

233 The first task to model is the motor decision-making task that involves reaching to either
 234 a single direction (instructed trial) or selecting between two opposite directions (choice

trial). Fig.5A illustrates the activity of the reach planning field as a function of time for a representative instructed (top panel) and choice (bottom panel) trial. Initially, the field activity is in the resting state. After the target onset in the choice trial, two neuronal populations selective for the targets are formed and compete through mutual inhibitory interactions. The activity of the pause field also increased to further inhibit the reach planning field to delay the initiation of the action (Fig. 6A blue trace shows the mean activity of the pause field across time in a choice trial). Once the activity of a neuronal population exceeds an action initiation threshold, the corresponding target is selected, the activity of the non-selected target is inhibited by the “winning” population, and a reaching movement is initiated. When only one target is presented (Fig.5A top panel), the activity of the corresponding neuronal population exceeds the action initiation threshold faster due to the lack of inhibitory competition from an alternative option and the non-activation of the pause field (Fig. 6A cyan trace shows that pause field activity remains on baseline). To get better insight on the model computations, consider two neurons in the choice trial, one from each population, centered at the target locations (Fig.5D). The neuron that exceeds the action initiation threshold first (red continuous traces) dictates the reaction time and the selected target (i.e., the selected direction of movement). In the absence of action competition (instructed trial), the activity of the reach neuron (blue trace) exceeds the action initiation threshold faster than when two actions compete for selection (red traces). Hence, we predict that simulated instructed reaches have shorter RT than reaches in the choice trials. To test this prediction, we simulated 100 decision-making trials in which 50 % of them involves choices between two competing options and the rest of them were instructed trials. Consistent with the prediction, we found that free choice movements have longer RT than instructed movements, as is shown in Fig.7A.

260 Figure 5 somewhere here

261

262

263 Figure 6 somewhere here

264

265 **2.3.2 Modeling the computations of conflicting information in motor deci-**

266 **sions**

267 In the Eriksen flanker task, a “flanker” (i.e., distractor) appears 100 ms before the target.

268 Once the flanker is presented and detected by the spatial sensory input field, a reach

269 neuronal population tuned to the flanker direction is formed - i.e., the model prepares

270 an action towards the direction of the flanker. If the upcoming target coincides with

271 the flanker direction (congruent trial), the pause field will not be activated (Fig.6B cyan

272 trace) and the activity of the reach neuronal population will be further increased, leading

273 to fast reaching movements towards the target direction (Fig.5B top panel). On the

274 other hand, if the target points to the opposite direction from the flanker (incongruent

275 trial), a new reach neuronal population is formed and competes with the reach neuronal

276 population of the flanker (Fig.5B bottom panel). The conflict signal field detects the

277 “conflicting information” and activates the pause field (Fig.6B blue trace) to suppress

278 the reach planning field so that the target population will have time to further increase

279 its activity and win the competition. The expected outcome field, which encodes the

280 correct movement direction, biases the competition towards the target direction. To better

281 understand the mechanism of action regulation in the Eriksen flanker task, we consider two

282 neurons centered at the location of the target and the distractor, respectively (Fig.5E). The

neuronal activity of the distractor (red discontinuous trace) increases before the neuronal activity of the target (red continuous trace), since distractor precedes target presentation. Once the target is cued, the two neurons compete through inhibitory interactions. This competition, as well as the inhibition of the reaching neuronal population from the pause field, delay the action initiation, leading to longer RT. On the other hand, the lack of action competition and the non-activation of the pause field in the congruent trials (Fig.6B cyan trace) lead to shorter RT. To test this prediction, we simulated 100 Eriksen flanker task trials with 50 % of them to be incongruent trials. Consistent with the prediction, we found that reaching movements in incongruent trials have longer RT than in congruent trials as illustrated in Fig. 7B.

2.3.3 Modeling the computations of outright stopping of actions

Regarding the stop-signal task, the model needs to generate actions while anticipating a stop signal. The experimental results showed that when people anticipate a stop signal, they have longer RT as compared to when they do not anticipate a stop signal (i.e., instructed trials). This suggests that the pause field is active even in the go trials to increase the chances of being able to abandon an action in case stopping is required. The reach planning field activity in the go task resembles that of an instructed trial in the decision-making task (Fig.5C top panel), the only difference being that in the go trials the pause field is continuously active (Fig.6C blue trace). Hence, the activity of the reach planning field increases slower compared to the instructed trial, resulting in longer RT. In a go trial, the reach neuronal population tuned to the target direction is formed preparing an action. Once the activity of the population exceeds an action initiation threshold, the action is performed. However, in some trials, a stop signal is cued and the pause field activity is further increased, which subsequently inhibits the activity of the

reach planning field to completely stop the planned or the ongoing action (Fig.5C bottom panel). To better understand the mechanism for stopping actions, consider one neuron from the population centered at the location of the target. The activity of the neuron increases once the target is cued and an action is initiated when the activity exceeds the action initiation threshold (Fig.5F blue trace). However, if a stop signal is cued, the pause field inhibits the activity of the neuron to stop the ongoing action (Fig.5F black trace). The stop signal is given with some delay (stop signal delay, SSD) in each trial. The longer the SSD is, the harder it is for the pause field to suppress the activity of the reach neuron increasing the chance to fail to stop the action. To test the model prediction, we simulated 50 go trials, as well as 250 stop trials, in which a stop stimulus appeared at different SSDs, signaling the model to abandon the action. Consistent with the model predictions, we found that go trials have longer RTs than instructed trials ($p < 0.001$, two-way ANOVA, comparison made between the mean RT on instructed trials in the decision-making task and mean RT on go trials in the stop-signal task), and the probability to successfully stop a response reduces with increased SSD - i.e., the longer the signal delay, the harder it is for the model to stop an action (Fig.8 blue trace).

2.4 Dysfunction of the pause mechanism predicts motor impairment in PD patients

So far the neurodynamical theory is capable of capturing the motor behavior of the neurotypical participants in the 3 action regulation tasks. However, one of the main findings in our study is that PD patients exhibit overall slower responses in nearly all tasks compared to neurotypical participants. This motor impairment can be explained within the neurodynamical theory as a deficit on the pause mechanism. That is, the

330 pause field is active even in the absence of conflicting information (congruent trials in
331 the Eriksen flanker task) or competition between multiple actions (instructed trials in
332 the decision-making task). To get a better understanding on how dysfunction of the
333 pause mechanism affects motor behavior, Fig.6 shows the activity of the pause field as a
334 function of time for a single trial across all tasks when simulating actions to model the
335 RT of neurotypical participants and PD patients. In the decision-making task, the pause
336 field is activated even when no action competition is presented (i.e., instructed trials)
337 to capture the RT of the PD patient (Fig.6A magenta trace). This explains the slower
338 response on initiating an action on instructed trials from PD patients. Also, the lack
339 of difference on RT between neurotypical and PD patients in free choice trials suggests
340 that the pause field exhibits similar activation levels when deciding between competing
341 options after targets onset in both groups (Fig.6A). Regarding the flanker task, the pause
342 field is active before the target onset in PD patients, explaining the slower response in
343 both congruent and incongruent trials compared to neurotypical individuals (Fig.6B red
344 and magenta traces). We need to point out here that although the pause field exhibits
345 the same activation level in instructed and free choice trials (decision-making task) in PD
346 patients, the slower response in choice trials compared to instructed trials is due to the
347 inhibitory action competition between the two alternative movement directions.

348 Additionally, another important finding in our study is that PD patients have shorter
349 RT in go trials than neurotypical participants in the stop signal task. By comparing
350 the RT of movements between go trials in the stop-signal task and instructed trials in
351 the decision-making task, we found that neurotypical participants delayed their responses
352 in the go trials because they anticipated a stop signal as compared to when they did
353 not anticipate a stop signal (i.e., instructed trials). This *response delay effect* (RDE)
354 has been reported in previous studies [47–50] and has been associated with an “active

braking mechanism” that increases the chance of abandoning a response in case stopping is required [51]. Note that PD patients also exhibited this active braking mechanism, but the difference in RT between go trials with anticipation of stopping signal and instructed trials was much smaller compared to neurotypical participants. Overall, these findings suggest that the pause field is active in the go trials for predicting the motor behavior in both groups of participants. In fact, the pause field activity is higher in neurotypical participants than PD patients, before a stop signal is detected, to explain the slower response of the first group compared to the latter group (Fig.6C, blue and red traces). We simulated 50 go trials with elevated pause field activity for both neurotypical participants and PD patients. Consistent with the behavioral findings, the go trials have longer RT in the simulated neurotypical participants than PD patients (Fig. 7C) ($p < 0.001$, two sample t-test). Additionally, the model predicts that the probability to successfully stop a response is lower in PD patients than in neurotypical individuals (Fig. 8) due to the faster response of PD patients.

Figure 7 somewhere here

Figure 8 somewhere here

3 Discussion

3.1 General

Survival of species in an ever-changing environment requires flexibility in action selection. Traditional theories suggest that action selection takes place before action preparation [52–55]. However, recent cognitive theories challenge this view suggesting that in situations affording more than one alternative options, individuals prepare multiple actions in parallel that compete for selection before choosing one to execute [6–10]. This theory received empirical support from neurophysiological investigations in the sensorimotor areas of non-human primates (NHPs) showing that the brain encodes parallel reach, grasp and saccade plans before the animals select between them [11,12,56]. It is consistent with the continuous flow model of perception, which suggests that response preparation can begin even before the goal is fully identified and a decision is made [14–16]. Psychophysical support for this theory comes from the observation that when reaching to multiple potential targets, the initial movement is directed towards the average location of the targets, consistent with the theory that multiple prepared reaches being executed simultaneously [17–19].

Flexibility in action selection includes not only being fast and accurate enough when selecting between competing options, but also being flexible enough to change actions according to updated demands of the environment. This includes delaying actions in the presence of conflicting information and completely abandoning obsolete actions when they are rendered inappropriate [57–60]. Series of studies have explored how different brain regions contribute to programming, re-programming and stopping of actions using neural recordings and functional neuroimaging techniques [20,21,24,25,28,29,61,62]. The basal ganglia (BG), and in particular, the subthalamic nucleus (STN), has been functionally

implicated in action regulation, but in association with distinct frontal areas, such as the primary motor cortex (M1), the premotor cortex (preMC), the presupplementary motor area (preSMA) and the right inferior frontal gyrus (rIFG) [31–34]. In a sense STN seems to act as a “brake” when a stop signal is presented to rapidly suppress ongoing actions. Furthermore, various computational theories including the drift-diffusion model (DDM), urgency-gating model (UGM), evidence accumulation models (EAMs), race models and mutual inhibition models, have been constructed to explain how the brain selects between competing options, inhibits actions in the presence of conflicting information and abandons planned or ongoing action when they are rendered inappropriate [63–66]. Although these theories provide significant insights into the action regulation mechanisms, a major limitation is that they explored separately each of these three motor functions, making it challenging to develop a unified theory of action regulation. A computational theory that can simulate the mechanisms underlying selecting, inhibiting and outright stopping of actions is needed to unify and integrate these distinctly studied actions and mechanisms.

Our research focuses exactly on what has been missing from previous studies – to design a large scale computational theory that can predict: 1) how the brain selects between competing actions, delays actions in the presence of conflicting information and stops actions when they are rendered inappropriate, 2) how neuropsychiatric diseases, such as PD, affect the action regulation circuitry and lead to motor deficits. Building on our previous work [38,39], we developed a neurodynamical framework to integrate the three action regulation functions into a unified computational theory. This computational theory is based on the affordance competition hypothesis, in which multiple actions are formed concurrently and compete over time until one has sufficient evidence to win the competition [6]. We replace evidence accumulation with desirability – a continuously evolving quantity that integrates all sources of information about the relative value of an

424 action with respect to alternatives. The winning action determines the reaction time and
 425 the direction of movement. The computational theory includes a BG-type mechanism
 426 of inhibiting actions in the presence of competing options, conflicting information and
 427 stopping signals. We tested the computational model in a series of tasks that involve
 428 action selection, decision conflict and outright stopping using neurotypical individuals
 429 and PD patients. Our findings showed that the model captures many aspects on human
 430 behavior, such as the longer RT in the presence of competing actions and conflicting
 431 information, as well as the inverse relationship between the probability to successfully
 432 stop an action and stop signal delay (SSD). It also predicts the motor impairment on PD
 433 patients when performing these three motor tasks as a deficit in the pause mechanism.
 434 In particular, the model explains the longer responses in generating actions even without
 435 the presence of competing action and conflicting information in PD patients compared
 436 to neurotypical participants as a consequence of hyperactivity on the pause field. This is
 437 consistent with experimental evidence showing that STN is overacting in PD patients [67]
 438 leading to longer responses in visuomotor tasks. Overall, to the best of our knowledge,
 439 our study presents the first neuro-computational theory that integrates the mechanisms
 440 of three action regulation functions and predicts how disruption of these mechanisms can
 441 lead to motor deficits reported in neurological diseases such as PD.

442 **3.2 Mapping to neurophysiology**

443 The computational theory presented in the current study is a systems-level framework
 444 aimed to qualitatively predict response patterns of neuronal activities in ensembles of
 445 neurons, as well as motor behavior, in action regulation tasks. It captures many key
 446 features of the functional properties of the cortical-subcortical network involved in action
 447 regulation. The spatial sensory input field mimics the organization level of the posterior

parietal cortex (PPC) [68, 69]. The expected reward field can be associated with the ventromedial prefrontal cortex (vmPFC) and orbitofrontal cortex (OFC), two frontal areas with important role in computation and integration of reward [70, 71]. The reach cost field can be equated to the anterior cingulate cortex (ACC) that has a key role in computing the cost for performing an action [72, 73]. The reach planning field can be associated with the parietal reach region (PRR) [74, 75] and the premotor dorsal cortex (PMd) [76, 77], two cortical areas involved in planning of reaching movements. The stop signal field can be equated with the right inferior frontal gyrus (rIFG), which is recruited when cues associated with response inhibition are detected [78, 79]. Regarding the conflict signal field, the popular view is that the pre-supplementary motor area (preSMA) detects the co-activation of different but conflicted responses (e.g., naming the color of the word *red* written with green color), it activates the STN to *temporarily* suppress a response [80, 81]. Finally the pause field can be equated to the STN which is activated in tasks that require stopping or pausing behavioral outputs to suppress actions [23, 27, 30, 35].

3.3 Computational modeling of action inhibition deficits in PD patients

PD is a progressive neurodegenerative disease associated with progressive loss of dopaminergic neurons in the substantia nigra of the BG [67]. The disruption of frontal-BG circuitry is responsible for the development of major symptoms of PD, including rigidity, tremor, bradykinesia, and postural instability [82, 83]. In particular, impairment of response inhibition abilities, which greatly affects the life quality of PD patients, is considered to be a sensitive measure to the progression of PD [84]. As a key player in the frontal-BG circuit, the STN is suggested to mediate a “pause” function by rapidly inhibiting the BG

activity. Therefore, it is considered to play a prominent role in the pathology of PD [85]. An increase in the neuronal activity of the STN has been demonstrated in electrophysiological and behavioral studies in non-human primate models of PD [86] as well as PD patients [87]. Our findings suggest that an increase in the STN-mediated “pause” signal is responsible for the impairment of action inhibition abilities in PD patients. In our model, we assigned higher baseline activation level of the pause field in the decision-making task and Eriksen flanker task in PD patients compared with neurotypical participants. Consistent with the model predictions, PD patients exhibited longer RT than healthy individuals in the instructed trials of the decision making task, as well as in both incongruent trials and congruent trials of the Eriksen flanker task. Notably, RT in the free choice trials of the decision-making task wasn’t significantly different between PD patients and neurotypical participants. This suggests that pause field, which is already highly active in instructed trials, is not further activated in the choice trials.

An interesting finding in our study was that neurotypical individuals had slower response than PD patients to initiate an action in the stop-signal task. This is somewhat counter-intuitive since the STN is overactive in PD patients and therefore we would expect that they would had slower response than neurotypical participants. However, when we compared RT between instructed trials (decision-making task) and go trials (stop signal task) of the neurotypical individuals, we found that they responded slower when they anticipated a stop signal. On the other hand, we found much subtler difference in RT between instructed trials and go trials in PD patients. This suggests that the pause mechanism is activated in the stop-signal task in neurotypical individuals even before a stop signal is presented. By activating the pause field to simulate the motor behavior of the neurotypical participants, the model predicts that PD patients will have faster responses and lower probability to stop planned or ongoing actions compared to neurotypical par-

496 ticipants. In other words, the model explains the slower responses of the neurotypical
497 participants as a cognitive strategy adapted to minimize the probability to fail to stop an
498 action if a stop signal is detected.

499 **3.4 Activity suppression or increase of action initiation thresh-** 500 **old?**

501 In our theory, the pause field delays motor decisions by suppressing the activity of the
502 reach planning field. However, an alternative hypothesis is that the pause field mediates
503 the action inhibition function by increasing the action initiation threshold. Previous
504 studies suggest that STN low-frequency oscillatory activity and medial prefrontal cortex
505 (mPFC)-STN coupling are involved in determining the amount of evidence (i.e., action
506 initiation threshold) needed before making a decision [88–91]. Additionally, clinical studies
507 showed that deep brain stimulation targeting the STN in PD patients can modulate the
508 amount of evidence, and therefore the action initiation threshold, required to initiate an
509 action [89]. Hence, it is also likely that the STN delays motor decisions in the presence
510 of competing actions and/or conflicting information by increasing the action initiation
511 threshold, instead of suppressing the activity of the motor areas that generate actions.
512 Our computational theory is capable of modeling this hypothesis by adjusting the action
513 initiation threshold in the reach planning field. However, it cannot dissociate between
514 the two hypotheses on how the STN pauses actions when needed. To do so, future
515 neurophysiological or neuroimaging studies need to record activity from the STN and
516 motor areas during decision tasks with multiple options and/or conflicting information.

517 **3.5 Hyperactive pause mechanism or altered cost/reward ratio** 518 **in PD patients?**

519 Although our study suggests that deficits in movement preparation in PD patients, such
520 as slow reaction times, are related to hyperactivity in STN that inhibits planned actions,
521 other studies have associated motor impairments with motivational deficits [92]. In partic-
522 ular, motivational deficits seem to significantly contribute to bradykinesia in PD patients
523 and lead to alternation in the amount of effort required to perform a movement at normal
524 speed, as well as the perceived reward for successfully completing the action [93].

525 Motor decisions are frequently made based on expected reward and the associated
526 effort cost required to obtain the reward. The cost has been considered to be detrimental,
527 since we tend to choose the less costly actions especially when they are associated with
528 similar expected rewards [94,95]. The dopaminergic neurons seem to be critically involved
529 in the process of cost versus reward (i.e., cost/reward ratio) evaluation. Dopamine deple-
530 tion from rat results in decreased tolerance for effort cost, whereas enhanced dopamine
531 levels has the opposite effect [94,96]. Loss of dopaminergic neurons and their projec-
532 tions is a major pathological hallmark in PD patients. Clinical studies have shown that
533 PD patients, regardless of medication status, tend to engage less effort for the lowest
534 reward compared with neurotypical participants in a hand-squeezing task [93]. However,
535 dopamine medication motivates PD patients to engage more effort for a given reward,
536 comparing to their off medication state. In addition, Deep brain stimulation (DBS) of
537 the STN establishes a reliable congruency between action and reward in PD patients and
538 remarkably enhances it over the level observed in neurotypical individuals [97].

539 Overall, these studies provide evidence that impairment of movement preparation in
540 PD patients can also be related to deficits in the mechanism that evaluates reward and

541 effort cost associated with actions - i.e., alternation of the cost/reward ratio. Notably,
 542 this can be also modeled within our neurodynamical framework by increasing the amount
 543 of effort required to perform actions towards the cued directions. Additionally, the alter-
 544 nation of the cost/reward ratio in PD patients could be also related to the hyperactivity of
 545 the STN - more effort is required to increase the activity of the motor population, which
 546 is continuously inhibited by the STN, to initiate an action. Today, the mechanism for
 547 motor and information processing deficits in PD patients is still under extensive study.
 548 PD is considered not only a disease caused by degeneration of substantia nigra dopamin-
 549 ergic neurons, but also a system-level disease caused by dysfunction of the cortical-BG
 550 circuit [67]. Therefore, both the hyperactivity of the STN and the altered cost/reward
 551 ratio can be considered parts of PD pathophysiology, and contribute to the motor deficits
 552 in PD patients.

553 3.6 Conclusions

554 In conclusion, the current study aims to advance our understanding on the computations
 555 underlying action regulations in tasks that involve action inhibition, the failure of which
 556 contributes to various neuropsychiatric diseases. We proposed a large scale neurodynam-
 557 ical computational framework that combines dynamic neural field theory with stochastic
 558 optimal control theory to simulate the mechanisms of action regulation and to predict
 559 how disruption of this mechanism lead to motor deficits in PD patients. We evaluated the
 560 model predictions by comparing the motor behavior of neurotypical individuals and PD
 561 patients in three tasks that require action inhibition. To the best of our knowledge, our
 562 results revealed for the first time an integrated mechanism of action regulation that affects
 563 both action planning and action inhibition. When this mechanism is disrupted (as in PD
 564 patients), motor behavior is affected, leading to longer reaction times and higher error

565 rates in decisions and actions. Overall, our findings provide significant insight on how the
566 brain regulates actions that involve inhibition, and open new avenues for improving and
567 developing therapeutic interventions for diseases that may involve these circuits.

568 4 Methods

569 4.1 Participants

570 A sample of 15 adults with PD and 32 neurologically healthy, age-matched adults took
571 part in the study. The study was approved by the University of California, Los Angeles
572 Review Board and all individuals signed an informed consent before participating.

573 4.2 Stimuli and Procedure

574 4.2.1 Decision-Making Task

575 All experiments were programmed using Psychtoolbox 3 for Matlab. Experimental setup
576 is shown in Figure 1. In the decision-making task, participants sat in a dark room in front
577 of a 22-inch Dell LED monitor where stimuli would be presented on. The screen was ap-
578 proximately 50 cm away from the participant. A two-dimensional joystick (Thrustmaster
579 T.16000M FCS, maximum range of axis value is $-32,000$ $+32,000$) was placed in front
580 of the monitor. During the task, the participants were instructed to move the joystick
581 towards the left or right direction using their right hand in reaction to the corresponding
582 stimulus. Each trial started with the screen turning black. After 1.0-1.1 s, a white fixation
583 cross appeared in the center of the black screen for 1.0-1.1 s, then the white fixation cross
584 disappeared, and four white arrows appear in the center of the black screen. In 50% of
585 the trials (choice trials), two of the arrows pointed to the left, and the other two to the

right (e.g. < < > >), in which case the participant needed to freely decide whether they would move the joystick to the left or right. In the other 50% of the trials (instructed trials), the four arrows were pointing to the same direction (left or right) (e.g. < < < <), in which case the participant needed to move the joystick towards the direction the arrows were pointing to. The arrows remained on the screen for up to 1.5 s before they disappear, then the screen turned black for 0.5 s. If the participant responded to the stimulus by moving the joystick to the left or right (axis value threshold for response: -25000 to the left/+25000 to the right) when the arrows were presented on the screen, after 10ms, the screen would turn black for the remaining of the 1.5 s plus 0.5 s, after which the screen would remain black and the next trial would start. If the joystick did not return to the baseline (axis value between -2500 and +2500), the next trial would not start until the joystick returned to the baseline. Every participant performed 2 blocks of trials, with 52 trials in each block. In each block of trials, there are 26 choice trials and 26 instructed trials. The trial type (choice or instructed) were randomized. Before each trial, the participant did not know whether the next trial would be a choice trial or an instructed trial. The RT for each trial was recorded as the time interval between the appearance of the arrows on the screen and the participant's response.

4.2.2 Eriksen flanker Task

An arrow version of the Eriksen flanker Task [98] with arrows pointing to the left and right was performed in our study. During the Eriksen Flanker task, the same equipment as described in 3.2.1 were used, the major difference being that in each trial, the target stimulus was flanked by stimuli which were pointing to the opposite direction of the target arrow (incongruent trial) or to the same direction as the target arrow (congruent trial), and every participant was told to move the joystick towards the same direction as the

target arrow using his/her right hand. In each trial, the screen first turned black for 1.0-1.1 s, then a white fixation cross appeared in the center of the screen for 1.0-1.1 s. After this interval, four white flanker arrows pointing to one direction (left or right) appeared in the center of the screen, leaving a blank space in the middle (e.g. < < < <). After 100 ms, a white target arrow appeared in the blank space, pointing either to the opposite direction of the flankers (incongruent trial) or the same direction (congruent trial). The target arrow and the flankers remained on the screen for up to 1.5 s, then disappeared, and the screen turned black for 0.5 s. If the participant responded to the target arrow by moving the joystick to the left or right, after 10ms, the screen would turn black for the remaining of the 1.5 s plus 0.5 s, after which if the joystick returned to baseline, the screen would remain black and start the next trial. Each participant performed two blocks of trials, with 52 trials in each block, making a total of 104 trials. In each block of trials, there are 26 incongruent trials and 26 congruent trials. The direction of the target arrows and the type of flanker (incongruent or congruent) were randomized. The RT for each trial was recorded as the time interval between the appearance of the target arrow and the participant's response.

4.2.3 Stop Signal Task

A trial in a stop signal task is either a go trial or a stop trial. In each trial, arrows pointing to the left or right direction were presented on the screen as a stimulus. In a go trial (no stop signal is presented), the participant should respond as fast as possible by moving the joystick towards the direction the arrows were pointing to. In a stop trial, the participant should try to inhibit their response after the stop signal was cued. Participants were told that stop was not always possible, and that stop trials and go trials are equally important. Before the experiment, each participant performed 24 training trials, including 16 go trials

and 8 stop trials. At the beginning of a trial, the screen turned black. After 1.0-1.1 s, a white fixation cross appeared in the center of the screen for 1.0-1.1 s, then the fixation cross disappeared, and four white arrows pointing to the left or right appeared in the center of the screen. In a go trial, the arrows remained on the screen for up to 1.5 s before they disappeared, then the screen turned black for 0.5 s. If the participant responded to the stimulus by moving the joystick when the arrows were presented on the screen, after 10ms, the screen turned black for the remaining of the 1.5 s plus 0.5 s, after which if the joystick returned to baseline, the screen remained black and the next trial was started. A stop trial is nearly identical to a go trial, except that the arrows turned red after an interval termed “stop signal delay” (SSD) indicating that the participant should abandon any response immediately. If the participant inhibited their actions, the arrows remained on the screen for the rest of 1.5 s, and in the subsequent stop trial, the SSD would increase by 50 ms, making inhibition more challenging. If the participant failed to inhibit their actions, after 10 ms, the arrows disappeared, and the screen turned black for the remaining of the 1.5 s plus 0.5 s, after which if the joystick returned to the baseline, the screen remained black and the next trial would start. In this case, the SSD would decrease by 50 ms, making it easier to inhibit actions. Each participant performed 3 blocks of trials, with 60 trials in each block. In each block of trials, there were 40 go trials and 20 stop trials. The direction of the arrows and the type of trial (go or stop) were randomized. The RT for each go trial and failed stop trial were recorded as the time interval between the appearance of white arrows and the participant’s response.

4.3 Statistical Analysis

Cubic interpolating splines were used to smooth the reach trajectories and compute the velocity of the movements. Reaction time (RT) was defined as the time between the target

appearance and the time that reach velocity exceeded 10% of the maximum velocity. RTs faster than 100ms were removed because anticipation is considered to be involved prior to actions, as well as RTs longer than 1500ms. RT outliers (RTs >3 standard deviations below or above the mean RT) were also excluded from the analysis. The trials in which the participant changed their mind (moving towards one direction past 5% of the maximum range, and then changed their mind to move towards the other direction) were also excluded from further analysis. RTs across all participants were pooled together, and for the decision making task and the Eriksen flanker task, two-way ANOVA analysis was performed to determine the group differences in RTs. For the stop signal task, two-sample t-test was performed to determine the group differences in go trial RTs.

4.4 Computational Model Architecture

We developed a neurodynamical framework based on our previous studies [38,39] to model the three action regulation functions. The computational framework combines dynamic neural field (DNF) theory with stochastic optimal control theory, and includes circuitry for perception, expected outcome, effort cost, context signal, pause, action planning and execution. Each DNF simulates the dynamic evolution of firing rate activity of a network of neurons over a continuous space with local excitation and surround inhibition. The functional properties of each DNF are determined by the lateral inhibition within the field and the connections with other fields in the architecture. The projections between the fields can be topologically organized – i.e., each neuron i in the field drives the activation at the corresponding neuron i in the other field (one-to-one connections), or unordered – i.e., each neuron in one field is connected with all neurons on the other field (one-to-all connections). The activity of a field j evolves over time under the influence of external inputs, local excitation and lateral inhibition interactions within the field, as well as

interactions with other k fields, as described by Equation (1):

$$\tau \dot{u}_j(x, t) = -u_j(x, t) + h_j + S_j(x, t) + [w_j \otimes f_j(u_j)](x, t) + \sum_k [w_{kj} \otimes f_k(u_k)](x, t) \quad (1)$$

where $u(x, t)$ is the local activity of the DNF at the position x and time t , and $\dot{u}_j(x, t)$ is the rate of change of the activity over time scale by a time constant τ . If there is no external input $S(x, t)$, the field converges over time to the resting state h from the current level of activation. The first convolution term $[w_j \otimes f_j(u_j)](x, t) = \int w(x - x') f[u(x', t)] dx'$ models interactions between the simulated neurons at different locations within the field j , and is shaped by the interaction kernel of Equation (2), which consists of both excitatory and inhibitory components:

$$w(x - x') = C_{exc} e^{-\frac{(x-x')^2}{2\sigma_{exc}^2}} - C_{inh} e^{-\frac{(x-x')^2}{2\sigma_{inh}^2}} \quad (2)$$

where C_{exc} , C_{inh} , σ_{exc} and σ_{inh} describe the amplitude and the width of the excitatory and the inhibitory components, respectively. We convolved the kernel function with a sigmoidal transformation of the field so that the neurons with activity above a threshold participate in the intra-field interactions:

$$f_j(u_j(x)) = \frac{1}{1 + e^{-\beta(u_j(x))}} \quad (3)$$

in which the steepness of the sigmoid function was controlled by β .

The function w_{jk} describes the connectivity kernel between fields u_j and u_k showing the contribution of field u_k to the dynamics of field u_j . The sigmoid $f_k(u_k)$ and w_{jk} are convolved to determine the full contribution from field u_k to u_j .

The architectural organization of the framework is shown in Figure 4. The “reach planning” field encodes the potential movement directions, and is responsible for initiating the reaching movements. The “spatial sensory input” field encodes the angular representations of the competing targets. The “expected outcome” field encodes the expected reward for reaching to a particular direction centered on the hand position. The outputs of these two fields send excitatory projections (green arrows) to the reach planning field in a topological manner. The “reach cost” field encodes the effort cost required to implement an action at a given time and state. The reach cost field sends inhibitory projections (red arrow) to the reach planning field to penalize high-effort actions. For instance, an action that requires changing of moving direction is more “costly” than an action of keep going in the same direction. The “pause” field suppresses the activity of the reach planning field to inhibit planned or ongoing actions via inhibitory projections to the reach planning field. The stop signal field and the conflict signal field encode information related to the contextual requirement of the task (i.e., stopping cue or flanker distractor), and send one-to-all excitatory projections to the corresponding population of the pause field. In particular, the stop signal field is projected to the neuronal population of the pause field which is responsible for outright stopping of action, whereas the conflict signal field projects to the neuronal population of the pause field, which is responsible for delaying decisions when conflicting information is detected. Each of the context signal fields (stop signal field and conflict signal field) consists of 100 neurons, whereas the pause field consists of 3 neuronal sub-populations, each consists of 75 neurons. The rest of the fields consist of 181 neurons with a preferred direction between 0 to 180 degrees. The activity of the reach planning field S_{action} is given as the sum of the outputs of the fields encoding the position of the target v_{pos} , the expected reward v_{reward} , the estimated reach cost v_{cost} , and the activity from the pause field v_{pau} , at any given time and state, corrupted by a

723 Gaussian distributed additive noise ξ .

$$S_{action} = \eta_{loc}v_{pos} + \eta_{reward}v_{reward} - \eta_{cost}v_{cost} - \eta_{pau}v_{pau} + \xi \quad (4)$$

724 where η_{loc} , η_{reward} , η_{cost} and η_{pau} are scalar values that weigh the influence of the
725 spatial sensory input field, the expected outcome field, the reach cost and the pause field,
726 respectively, to the activity of the reach planning field. The values of the model parameters
727 are given in S1 Table. The normalized activity of the reach planning field describes the
728 relative desirability d_i of each “reach neuron” with respect to the alternative options at
729 time t – i.e., the higher the activity of a reach neuron j , the higher the desirability to
730 move towards the preferred direction φ_j of this neuron with respect to the alternatives
731 at a given time t . Each neuron j in the reach planning field is connected with a control
732 scheme that generates reaching trajectories. Once the activity of that neuron exceeds the
733 action initiation threshold γ , the controller is triggered and generates an optimal policy
734 π_j , a sequence of motor actions towards the preferred direction of the neuron j . The
735 optimal policy is given by minimization of the cost function:

$$J_j(\mathbf{x}_t, \pi_j) = (\mathbf{x}_{T_j} - S\mathbf{p}_j)^T Q_{T_j} (\mathbf{x}_{T_j} - S\mathbf{p}_j) + \sum_{t=1}^{T_j-1} \pi_j(\mathbf{x}_t)^T R \pi_j(\mathbf{x}_t) \quad (5)$$

736 where $\pi_j(\mathbf{x}_t)$ is the policy from the time $t = 1$ to $t = T_j$ to reach towards the preferred
737 direction φ_j ; T_j is the time required to arrive at position \mathbf{p}_j ; \mathbf{p}_j is the position planned
738 to arrive (goal position) at the end of the reaching movement, given by $\mathbf{p}_j = [\text{rcos}(\varphi_j),$
739 $\text{rsin}(\varphi_j)]$, in which r is the distance between the current location of the hand and the
740 location of the stimulus encoded by the neuron j . \mathbf{x}_{T_j} is the state vector at the end of
741 the reaching movement, and matrix S selects the actual position of the hand and the goal
742 position at the end of the reaching movement from the state vector. Matrices Q_{T_j} and R

define the cost dependent on precision and control, respectively. More details about the optimal control model are described in [38,39]. Consequently, a action is initiated once a neuronal population exceeds the action initiation threshold and the executed action $\pi_{mix}(\mathbf{x}_t)$ is given as a mixture of the active policies (i.e., policies with active neurons) weighted by relative desirability values of the corresponding neurons at any given time and state.

$$\pi_{mix}(\mathbf{x}_t) = \sum_j^{j+M} d_j(\mathbf{x}_t) \pi_j(\mathbf{x}_t) \quad (6)$$

where \mathbf{x}_t is the state of the system at time t (i.e., position, velocity, orientation of the trajectory), d_j is the normalized activity of the neuron j (i.e., relative desirability value of the neuron j), and π_j is the optimal policy generated by the controller connected with neuron j . Because desirability is time- and state-dependent, the weighted mixture of the individual policies can change/correct the current trajectory in the presence of new incoming information - e.g., a stop signal cued while acting. In order to handle contingencies during the movement, the “receding horizon control”(RHC) [99,100] technique, also known as model predictive control (MPC), which is widely used in stochastic optimal control models, was implemented in the framework. According to RHC, the framework would only execute the initial portion of the sequence of actions for a short period of time τ ($\tau = 9$ in our framework), after which the framework would recompute the optimal policy $\pi_{mix}(\mathbf{x}_t + \tau)$ from time $t+\tau$ to $t+\tau+T_i$, and this approach would continue until the hand reaches one of the targets.

762 Acknowledgments

763 Research reported in this publication was supported by National Institute of Neurological
764 Disease and Stroke of the National Institutes of Health under award number U01NS098961
765 and R01NS097782. The content is solely the responsibility of the authors and does not
766 necessarily represent the official views of the National Institutes of Health.

767 Author Contributions

768 N.P. and V.N.C conceived the study.; J.C., M.M, N.P. and V.N.C designed the exper-
769 iment; N.H., D.B. and M.M. recruited subjects and collected the data; S.Z. and J.C.
770 performed the data analysis; S.Z designed the neurocomputational model and performed
771 the simulations; S.Z drafted the manuscript with substantial contribution from N.P. and
772 V.N.C; S.Z, J.C., N.P. and V.N.C. revised and approved the manuscript.

773 Data Availability

774 All relevant data are within the manuscript and its supporting information files and will
775 be uploaded to the Open Science Framework (OSF) upon approval for publication.

776 References

- 777 1. Gauggel S, Rieger M, and Feghoff TA. Inhibition of ongoing responses in pa-
778 tients with parkinson's disease. *Journal of Neurology, Neurosurgery & Psychiatry*,
779 75(4):539–544, 2004.

- 780 2. Wylie SA, van den Wildenberg WPM, Ridderinkhof KR, Bashore TR, Powell VD,
781 Manning CA, and Wooten GF. The effect of parkinson's disease on interference
782 control during action selection. *Neuropsychologia*, 47(1):145–157, 2009.
- 783 3. Yaniv A, Benaroya-Milshtein N, Steinberg T, Ruhrrman D, Apter A, and Lavidor
784 M. Specific executive control impairments in tourette syndrome: The role of
785 response inhibition. *Research in developmental disabilities*, 61:1–10, 2017.
- 786 4. Morein-Zamir S, Fineberg NA, Robbins TW, and Sahakian BJ. Inhibition of
787 thoughts and actions in obsessive-compulsive disorder: extending the endopheno-
788 type? *Psychological medicine*, 40(2):263–272, 2010.
- 789 5. van Velzen LS, Vriend C, de Wit SJ, and van den Heuvel OA. Response inhibition
790 and interference control in obsessive–compulsive spectrum disorders. *Frontiers in*
791 *human neuroscience*, 8:419, 2014.
- 792 6. Cisek P. Cortical mechanisms of action selection: the affordance competition
793 hypothesis. *Philosophical Transactions of the Royal Society B: Biological Sciences*,
794 362(1485):1585–1599, 2007.
- 795 7. Cisek P and Kalaska JF. Neural mechanisms for interacting with a world full of
796 action choices. *Annual review of neuroscience*, 33:269–298, 2010.
- 797 8. Gallivan JP, Barton KS, Chapman CS, Wolpert DM, and Flanagan JR. Action
798 plan co-optimization reveals the parallel encoding of competing reach movements.
799 *Nature communications*, 6(1):1–9, 2015.
- 800 9. Gallivan JP, Logan L, Wolpert DM, and Flanagan JR. Parallel specification of
801 competing sensorimotor control policies for alternative action options. *Nature*
802 *neuroscience*, 19(2):320, 2016.

- 803 10. Gallivan JP, Chapman CS, Wolpert DM, and Flanagan JR. Decision-making in
804 sensorimotor control. *Nature Reviews Neuroscience*, 19(9):519–534, 2018.
- 805 11. McPeck RM, Han JH, and Keller EL. Competition between saccade goals in
806 the superior colliculus produces saccade curvature. *Journal of neurophysiology*,
807 89(5):2577–2590, 2003.
- 808 12. Cisek P and Kalaska JF. Neural correlates of reaching decisions in dorsal premotor
809 cortex: specification of multiple direction choices and final selection of action.
810 *Neuron*, 45(5):801–814, 2005.
- 811 13. Baumann MA, Fluet MC, and Scherberger H. Context-specific grasp movement
812 representation in the macaque anterior intraparietal area. *Journal of Neuroscience*,
813 29(20):6436–6448, 2009.
- 814 14. Eriksen CW and Schultz DW. Information processing in visual search: A con-
815 tinuous flow conception and experimental results. *Perception & psychophysics*,
816 25(4):249–263, 1979.
- 817 15. Miller J. Discrete versus continuous stage models of human information process-
818 ing: in search of partial output. *Journal of Experimental Psychology: Human*
819 *Perception and Performance*, 8(2):273, 1982.
- 820 16. Gratton G, Coles MG, Sirevaag EJ, Eriksen CW, and Donchin E. Pre-and post-
821 stimulus activation of response channels: a psychophysiological analysis. *Journal*
822 *of Experimental Psychology: Human perception and performance*, 14(3):331, 1988.
- 823 17. Chapman CS, Gallivan JP, Wood DK, Milne JL, Culham JC, and Goodale MA.
824 Reaching for the unknown: multiple target encoding and real-time decision-
825 making in a rapid reach task. *Cognition*, 116(2):168–176, 2010.

- 826 18. Chou IH, Sommer MA, and Schiller PH. Express averaging saccades in monkeys.
827 *Vision research*, 39(25):4200–4216, 1999.
- 828 19. Enachescu V, Schrater P, Schaal S, and Christopoulos V. Action planning and con-
829 trol under uncertainty emerge through a desirability-driven competition between
830 parallel encoding motor plans. *PLoS computational biology*, 17(10):e1009429, 2021.
- 831 20. Mars RB, Piekema C, Coles MG, Hulstijn W, and Toni I. On the programming
832 and reprogramming of actions. *Cerebral Cortex*, 17(12):2972–2979, 2007.
- 833 21. Li CS, Huang C, Constable RT, and Sinha R. Imaging response inhibition in
834 a stop-signal task: neural correlates independent of signal monitoring and post-
835 response processing. *Journal of Neuroscience*, 26(1):186–192, 2006.
- 836 22. Ray NJ, Brittain JS, Holland P, Joundi RA, Stein JF, Aziz TZ, and Jenkinson
837 N. The role of the subthalamic nucleus in response inhibition: evidence from
838 local field potential recordings in the human subthalamic nucleus. *Neuroimage*,
839 60(1):271–278, 2012.
- 840 23. Wessel JR, Jenkinson N, Brittain JS, Voets SH, Aziz TZ, and Aron AR. Sur-
841 prise disrupts cognition via a fronto-basal ganglia suppressive mechanism. *Nat*
842 *Commun.*, 7, 2016.
- 843 24. González-Villar AJ, Bonilla FM, and Carrillo de-la Peña MT. When the brain
844 simulates stopping: neural activity recorded during real and imagined stop-signal
845 tasks. *Cognitive, Affective, & Behavioral Neuroscience*, 16(5):825–835, 2016.
- 846 25. Wagner J, Wessel JR, Ghahremani A, and Aron AR. Establishing a right frontal
847 beta signature for stopping action in scalp eeg: implications for testing inhibitory

- control in other task contexts. *Journal of cognitive neuroscience*, 30(1):107–118,
2018.
26. Bastin J, Polosan M, Benis D, Goetz L, Bhattacharjee M, Piallat B, Krainik A,
Bougerol T, Chabardes S, and David O. Inhibitory control and error monitoring
by human subthalamic neurons. *Transl Psychiatry*, 4(9), 2014.
27. Benis D, David O, Piallat B, Kibleur A, Goetz L, Bhattacharjee M, Fraix V,
Seigneuret E, Krack P, Chabardes S, and Bastin J. Response inhibition rapidly in-
creases single-neuron responses in the subthalamic nucleus of patients with parkin-
son’s disease. *Cortex*, 84:111–123, 2016.
28. Chen X, Scangos KW, and Stuphorn V. Supplementary motor area exerts
proactive and reactive control of arm movements. *Journal of Neuroscience*,
30(44):14657–14675, 2010.
29. Pani P, Giarrocco F, Giamundo M, Montanari R, Brunamonti E, and Ferraina
S. Visual salience of the stop signal affects the neuronal dynamics of controlled
inhibition. *Scientific reports*, 8(1):1–13, 2018.
30. Schmidt R, Leventhal DK, Mallet N, Chen F, and Berke JD. Canceling actions
involves a race between basal ganglia pathways. *Nat Neurosci.*, 16(8):1118–1124,
2013.
31. Parent A and Hazrati LN. Functional anatomy of the basal ganglia. i. the cortico-
basal ganglia-thalamo-cortical loop. *Brain research reviews*, 20(1):91–127, 1995.
32. Aron AR, Fletcher PC, Bullmore ET, Sahakian BJ, and Robbins TW. Stop-signal
inhibition disrupted by damage to right inferior frontal gyrus in humans. *Nature
neuroscience*, 6(2):115–116, 2003.

- 871 33. Chambers CD, Bellgrove MA, Stokes MG, Henderson TR, Garavan H, Robertson
872 IH, Morris AP, and Mattingley JB. Executive “brake failure” following deacti-
873 vation of human frontal lobe. *Journal of cognitive neuroscience*, 18(3):444–455,
874 2006.
- 875 34. Haynes WI and Haber SN. The organization of prefrontal-subthalamic inputs
876 in primates provides an anatomical substrate for both functional specificity and
877 integration: implications for basal ganglia models and deep brain stimulation.
878 *Journal of Neuroscience*, 33(11):4804–4814, 2013.
- 879 35. Aron AR and Poldrack RA. Cortical and subcortical contributions to stop signal
880 response inhibition: role of the subthalamic nucleus. *Journal of Neuroscience*,
881 26(9):2424–2433, 2006.
- 882 36. Aron AR, Behrens TE, Smith S, Frank MJ, and Poldrack RA. Triangulating
883 a cognitive control network using diffusion-weighted magnetic resonance imaging
884 (mri) and functional mri. *Journal of Neuroscience*, 27(14):3743–3752, 2007.
- 885 37. Rae CL, Hughes LE, Anderson MC, and Rowe JB. The prefrontal cortex achieves
886 inhibitory control by facilitating subcortical motor pathway connectivity. *Journal*
887 *of neuroscience*, 35(2):786–794, 2015.
- 888 38. Christopoulos V, Bonaiuto J, and Andersen RA. A biologically plausible computa-
889 tional theory for value integration and action selection in decisions with competing
890 alternatives. *PLoS Comput Biol*, 11(3):e1004104, 2015.
- 891 39. Christopoulos V and Schrater PR. Dynamic integration of value information into
892 a common probability currency as a theory for flexible decision making. *PLoS*
893 *Comput Biol*, 11(9):e1004402, 2015.

- 894 40. Luce RD et al. *Response times: Their role in inferring elementary mental orga-*
895 *nization*. Number 8. Oxford University Press on Demand, 1986.
- 896 41. Ramautar JR, Kok A, and Ridderinkhof KR. Effects of stop-signal probability
897 in the stop-signal paradigm: The n2/p3 complex further validated. *brain and*
898 *cognition. Brain Cogn.*, 56(2):234–252, 2004.
- 899 42. Van de Laar MC, Wildenberg WP, Boxtel GJ, and MW Molen. Processing of
900 global and selective stop signals: Application of donders’ subtraction method to
901 stop-signal task performance. *Exp Psychol.*, 57(2):149–159, 2010.
- 902 43. Sandamirskaya Y. Dynamic neural fields as a step toward cognitive neuromorphic
903 architectures. *Frontiers in Neuroscience*, 7(276), 2014.
- 904 44. Knips G, Zibner SK, Reimann H, and Schöner G. A neural dynamics architecture
905 for grasping that integrates perception and movement generation and enables on-
906 line updating. *Frontiers in neurorobotics*, 11(9), 2017.
- 907 45. Todorov E. Stochastic optimal control and estimation methods adapted to the
908 noise characteristics of the sensorimotor system. *Neural computation*, 17(5):1084–
909 1108, 2005.
- 910 46. Diedrichsen J, Shadmehr R, and Ivry RB. The coordination of movement: optimal
911 feedback control and beyond. *Trends Cogn Sci.*, 14(1):31–39, 2010.
- 912 47. Verbruggen F and Logan GD. Response inhibition in the stop-signal paradigm.
913 *Trends in cognitive sciences*, 12(11):418–424, 2008.
- 914 48. Verbruggen F and Logan GD. Proactive adjustments of response strategies in the
915 stop-signal paradigm. *J Exp Psychol Hum Percept Perform.*, 35(3):835–854, 2009.

- 916 49. Zandbelt BB, Bloemendaal M, Neggers SF, Kahn RS, and Vink M. Expectations
917 and violations: delineating the neural network of proactive inhibitory control.
918 *Hum Brain Mapp.*, 34(9):2015–2024, 2013.
- 919 50. Verbruggen F, Aron AR, Band GP, Beste C, Bissett PG, Brockett AT, Brown JW,
920 Chamberlain SR, Chambers CD, Colonius H, Colzato LS, Corneil BD, Coxon JP,
921 Dupuis A, Eagle DM, Garavan H, Greenhouse I, Heathcote A, Huster RJ, Jahfari
922 S, Kenemans JL, Leunissen I, Li CR, Logan GD, Matzke D, Morein-Zamir S,
923 Murthy A, Paré M, Poldrack RA, Ridderinkhof KR, Robbins TW, Roesch M,
924 Rubia K, Schachar RJ, Schall JD, Stock AK, Swann NC, Thakkar KN, van der
925 Molen MW, Vermeylen L, Vink M, Wessel JR, Whelan R, Zandbelt BB, and
926 Boehler CN. A consensus guide to capturing the ability to inhibit actions and
927 impulsive behaviors in the stop-signal task. *Elife*, 8(e46323), 2019.
- 928 51. Jahfari S, Stinear CM, Claffey M, Verbruggen F, and Aron AR. Responding
929 with restraint: what are the neurocognitive mechanisms? *J Cogn Neurosci.*,
930 22(7):1479–1492, 2010.
- 931 52. Padoa-Schioppa C and Assad JA. Neurons in the orbitofrontal cortex encode
932 economic value. *Nature*, 441(7090):223–226, 2006.
- 933 53. Padoa-Schioppa C. Neurobiology of economic choice: a good-based model. *Annual*
934 *review of neuroscience*, 34:333–359, 2011.
- 935 54. Tversky A and Kahneman D. The framing of decisions and the psychology of
936 choice. *science*, 211(4481):453–458, 1981.

- 937 55. Cai X and Padoa-Schioppa C. Neuronal encoding of subjective value in dorsal
938 and ventral anterior cingulate cortex. *Journal of Neuroscience*, 32(11):3791–3808,
939 2012.
- 940 56. Baumann MA, Fluet MC, and Scherberger H. Context-specific grasp move-
941 ment representation in the macaque anterior intraparietal area. *J Neurosci.*,
942 29(20):6436–48, 2009.
- 943 57. Archambault PS, Ferrari-Toniolo S, and Battaglia-Mayer A. Online control of
944 hand trajectory and evolution of motor intention in the parietofrontal system.
945 *Journal of Neuroscience*, 31(2):742–752, 2011.
- 946 58. Boucher L, Palmeri TJ, Logan GD, and Schall JD. Inhibitory control in mind
947 and brain: an interactive race model of countermanding saccades. *Psychological*
948 *review*, 114(2):376, 2007.
- 949 59. Orban de Xivry JJ and Lefèvre P. A switching cost for motor planning. *Journal*
950 *of neurophysiology*, 116(6):2857–2868, 2016.
- 951 60. Logan GD and Cowan WB. On the ability to inhibit thought and action: A theory
952 of an act of control. *Psychological review*, 91(3):295, 1984.
- 953 61. Swann N, Tandon N, Canolty R, Ellmore TM, McEvoy LK, Dreyer S, DiSano
954 M, and Aron AR. Intracranial eeg reveals a time-and frequency-specific role for
955 the right inferior frontal gyrus and primary motor cortex in stopping initiated
956 responses. *Journal of Neuroscience*, 29(40):12675–12685, 2009.
- 957 62. Wessel JR, Conner CR, Aron AR, and Tandon N. Chronometric electrical stim-
958 ulation of right inferior frontal cortex increases motor braking. *Journal of Neuro-*
959 *science*, 33(50):19611–19619, 2013.

- 960 63. Thura D, Beauregard-Racine J, Fradet CW, and Cisek P. Decision making by
961 urgency gating: theory and experimental support. *Journal of neurophysiology*,
962 108(11):2912–2930, 2012.
- 963 64. Krajbich I and Rangel A. Multialternative drift-diffusion model predicts the rela-
964 tionship between visual fixations and choice in value-based decisions. *Proceedings*
965 *of the National Academy of Sciences*, 108(33):13852–13857, 2011.
- 966 65. Vickers D and Smith P. Accumulator and random-walk models of psychophysical
967 discrimination: a counter-evaluation. *Perception*, 14(4):471–497, 1985.
- 968 66. Edwards DH. Mutual inhibition among neural command systems as a possible
969 mechanism for behavioral choice in crayfish. *Journal of Neuroscience*, 11(5):1210–
970 1223, 1991.
- 971 67. Alexander GE. Biology of parkinson’s disease: pathogenesis and pathophysiology
972 of a multisystem neurodegenerative disorder. *Dialogues in clinical neuroscience*,
973 6(3):259, 2004.
- 974 68. Andersen RA and Cui H. Intention, action planning, and decision making in
975 parietal-frontal circuits. *Neuron*, 63(5):568–583, 2009.
- 976 69. Hadjidimitrakis K, Bakola S, Wong YT, and Hagan MA. Mixed spatial and
977 movement representations in the primate posterior parietal cortex. *Front Neural*
978 *Circuits*, 13(15), 2019.
- 979 70. Padoa-Schioppa C and Assad JA. Neurons in the orbitofrontal cortex encode
980 economic value. *Nature*, 441(7090):223–226, 2006.

- 981 71. O'Doherty JP. Contributions of the ventromedial prefrontal cortex to goal-directed
982 action selection. *Annals of the New York Academy of Sciences*, 1239(1):118–129,
983 2011.
- 984 72. Rudebeck PH, Behrens TE, Kennerley SW, Baxter MG, Buckley MJ, Walton
985 ME, and Rushworth MFS. Frontal cortex subregions play distinct roles in choices
986 between actions and stimuli. *J Neurosci.*, 28(51):13775–13785, 2008.
- 987 73. Wallis JD and Kennerley SW. Heterogeneous reward signals in prefrontal cortex.
988 *Curr Opin Neurobiol.*, 20(2):191–198, 2010.
- 989 74. Snyder LH, Batista AP, and Andersen RA. Coding of intention in the posterior
990 parietal cortex. *Curr Opin Neurobiol.*, 386(6621):167–70, 1997.
- 991 75. Batista AP, Buneo CA, Snyder LH, and Andersen RA. Reach plans in eye-centered
992 coordinates. *Science*, 285(5425):257–260, 1999.
- 993 76. Pastor-Bernier A and Cisek P. Neural correlates of biased competition in premotor
994 cortex. *J Neurosci.*, 31(19):7083–7088, 2011.
- 995 77. Pastor-Bernier A, Tremblay E, and Cisek P. Dorsal premotor cortex is involved
996 in switching motor plans. *Front. Neuroeng.*, 5(5), 2012.
- 997 78. Aron AR, Robbins TW, and Poldrack RA. Inhibition and the right inferior frontal
998 cortex. *Trends Cogn Sci.*, 8(4):170–177, 2004.
- 999 79. Hampshire A, Chamberlain SR, Monti MM, Duncan J, and Owen AM. The role
1000 of the right inferior frontal gyrus: inhibition and attentional control. *NeuroImage*,
1001 50(3):1313–9, 2010.

- 1002 80. Wiecki TV and Frank MJ. A computational model of inhibitory control in frontal
1003 cortex and basal ganglia. *Psychological review*, 120(2):329, 2013.
- 1004 81. Zavala B, Zaghloul K, and Brown P. The subthalamic nucleus, oscillations, and
1005 conflict. *Mov Disord.*, 30(3):328–338, 2015.
- 1006 82. Hess CW and Hallett M. The phenomenology of parkinson’s disease. In *Seminars*
1007 *in neurology*, volume 37, page 109. NIH Public Access, 2017.
- 1008 83. Borriane P, Tranchita E, Sansone P, and Parisi A. Effects of physical activity in
1009 parkinson’s disease: A new tool for rehabilitation. *World Journal of Methodology*,
1010 4(3):133, 2014.
- 1011 84. Harrington DL, Shen Q, Theilmann RJ, Castillo GN, Litvan I, Filoteo JV, Huang
1012 M, and Lee RR. Altered functional interactions of inhibition regions in cognitively
1013 normal parkinson’s disease. *Frontiers in aging neuroscience*, 10:331, 2018.
- 1014 85. Brittain JS, Watkins KE, Joundi RA, Ray NJ, Holland P, Green AL, Aziz TZ,
1015 and N Jenkinson. A role for the subthalamic nucleus in response inhibition during
1016 conflict. *Journal of Neuroscience*, 32(39):13396–13401, 2012.
- 1017 86. Miller WC and DeLong MR. Altered tonic activity of neurons in the globus
1018 pallidus and subthalamic nucleus in the primate mptp model of parkinsonism. In
1019 *The basal ganglia II*, pages 415–427. Springer, 1987.
- 1020 87. Remple MS, Bradenham CH, Kao CC, Charles PD, Neimat JS, and Konrad PE.
1021 Subthalamic nucleus neuronal firing rate increases with parkinson’s disease pro-
1022 gression. *Movement Disorders*, 26(9):1657–1662, 2011.

- 1023 88. Bogacz R, Brown E, Moehlis J, Holmes P, and Cohen JD. The physics of optimal
1024 decision making: a formal analysis of models of performance in two-alternative
1025 forced-choice tasks. *Psychological review*, 113(4):700, 2006.
- 1026 89. Frank MJ. Hold your horses: a dynamic computational role for the subthalamic
1027 nucleus in decision making. *Neural networks*, 19(8):1120–1136, 2006.
- 1028 90. Cavanagh JF, Wiecki TV, Cohen MX, Figueroa CM, Samanta J, Sherman SJ,
1029 and Frank MJ. Subthalamic nucleus stimulation reverses mediofrontal influence
1030 over decision threshold. *Nature neuroscience*, 14(11):1462–1467, 2011.
- 1031 91. Herz DM, Zavala BA, Bogacz R, and Brown P. Neural correlates of decision
1032 thresholds in the human subthalamic nucleus. *Current Biology*, 26(7):916–920,
1033 2016.
- 1034 92. Mazzoni P, Hristova A, and Krakauer JW. Why don’t we move faster? parkin-
1035 son’s disease, movement vigor, and implicit motivation. *Journal of neuroscience*,
1036 27(27):7105–7116, 2007.
- 1037 93. Chong TT, Bonnelle V, Manohar S, Veromann KR, Muhammed K, Tofaris GK,
1038 Hu M, and Husain M. Dopamine enhances willingness to exert effort for reward
1039 in parkinson’s disease. *cortex*, 69:40–46, 2015.
- 1040 94. Salamone JD, Correa M, Farrar A, and Mingote SM. Effort-related functions of
1041 nucleus accumbens dopamine and associated forebrain circuits. *Psychopharma-*
1042 *cology*, 191(3):461–482, 2007.
- 1043 95. Walton ME, Kennerley SW, Bannerman DM, Phillips PE, and Rushworth MF.
1044 Weighing up the benefits of work: behavioral and neural analyses of effort-related
1045 decision making. *Neural networks*, 19(8):1302–1314, 2006.

- 1046 96. Salamone JD and Correa M. Motivational views of reinforcement: implications
1047 for understanding the behavioral functions of nucleus accumbens dopamine. *Be-*
1048 *havioural brain research*, 137(1-2):3–25, 2002.
- 1049 97. Wagenbreth C, Zaehle T, Galazky I, Voges J, Guitart-Masip M, Heinze HJ, and
1050 Düzel E. Deep brain stimulation of the subthalamic nucleus modulates reward
1051 processing and action selection in parkinson patients. *Journal of Neurology*,
1052 262(6):1541–1547, 2015.
- 1053 98. Eriksen BA and Eriksen CW. Effects of noise letters upon the identification of
1054 a target letter in a nonsearch task. *Perception & psychophysics*, 16(1):143–149,
1055 1974.
- 1056 99. Mayne DQ, Rawlings JB, Rao CV, and Scokaert POM. Constrained model pre-
1057 dictive control: Stability and optimality. *Automatica*, 36(6):789–814, 2000.
- 1058 100. Goodwin G, Seron MM, and De Doná JA. *Constrained control and estimation:*
1059 *an optimisation approach*. Springer Science & Business Media, 2006.

1060 Figure Legends

1061 **Fig.1 Experimental setup for action regulation tasks that require action inhi-**
1062 **bition.**(A) Decision-making task, including instructed and choice trials. (B) An arrow
1063 version of the Eriksen Flanker task, including congruent (the flanker arrows point to the
1064 same direction as the central arrow) and incongruent (the flanker arrows point to the
1065 opposite direction from the central arrow) trials. (C) A stop-signal task with instructed
1066 trials. Individuals are prompted to stop the action when the arrows turn red.

1067

Fig.2 Behavioral findings from the decision-making task, the Eriksen flanker task and the stop-signal task. (A) Bar plots of the RT for neurotypical individuals (Neurotypical) and PD patients (PD) in the instructed and choice trials of the decision-making task. Error bars correspond to standard error (SE). (B) Bar plots of the RT for neurotypical individuals (Neurotypical) and PD patients (PD) in the congruent and incongruent trials of the Eriksen flanker task. Error bars correspond to standard error (SE). (C) Bar plots of the RT for neurotypical individuals (Neurotypical) and PD patients (PD) in the go trials of the stop-signal task. Error bars correspond to standard error (SE).

Fig.3 Probability to successfully stop an action as a function of the stop signal delay (SSD). The probability to successfully stop an action as a function of the SSD for neurotypical individuals (Neurotypical,blue) and PD patients (PD,red).

Fig.4 Model Architecture. The architectural organization of the neurodynamical theory to model tasks that involve action inhibition, such as decisions between competing options, decisions in the presence of conflicting information and outright stopping of actions.

Fig.5 Simulated reach planning field neuronal activity changes in the decision making task, Eriksen flanker task and stop-signal task (A)-(C) Activity changes of the 181 neurons in the reach planning field during the decision making task (instructed trial and choice trial)(A), the Eriksen flanker task (incongruent trial and congruent trial)(B), and the stop-signal task (go trial and stop trial)(C) .(D)-(F) Activity changes of single neurons in the reach planning field during the decision making task(D), the Eriksen flanker task(E), and the stop-signal task(F).

Fig.6 Simulated behavioral results from the three tasks. Simulated reaction time (RT) for the three experimental tasks predicted by the neurodynamical theory for both neurotypical individuals (Neurotypical, blue) and PD patients (PD, red).

Fig.7 Simulated pause field activity changes during the three tasks (A) Activity changes of single neuron in the pause field during the decision making-task. Cyan trace, simulated pause field activity during an instructed trial for a neurotypical individual. Magenta trace, simulated pause field activity during an instructed trial for a PD patient. Blue trace, simulated pause field activity during a choice trial for a neurotypical individual. Red trace, simulated pause field activity during a choice trial for a PD patient. (B) Activity changes of single neuron in the pause field during the Eriksen flanker task. Cyan trace, simulated pause field activity during a congruent trial for a neurotypical individual. Magenta trace, simulated pause field activity during a congruent trial for a PD patient. Blue trace, simulated pause field activity during an incongruent trial for a neurotypical individual. Red trace, simulated pause field activity during an incongruent trial for a PD patient. (C) Activity changes of single neuron in the pause field during the stop-signal task. Blue trace, simulated pause field activity during a stop trial for a neurotypical individual. Red trace, simulated pause field activity during a stop trial for a PD patient.

Fig. 8 Simulated probability to successfully stop an action as a function of the stop signal delay (SSD) The (simulated) probability to successfully stop an action as a function of the SSD for neurotypical individuals (Neurotypical,blue) and PD patients (PD,red).

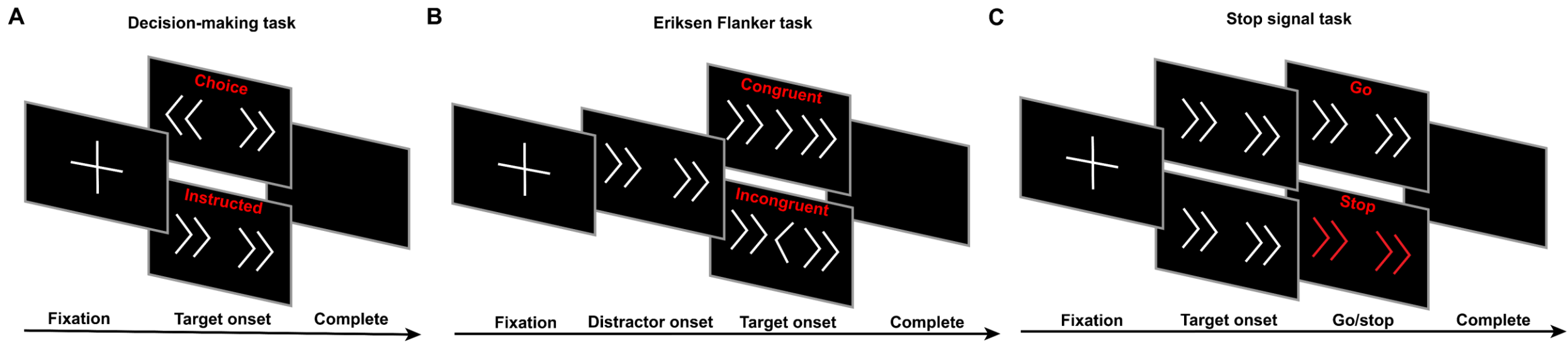
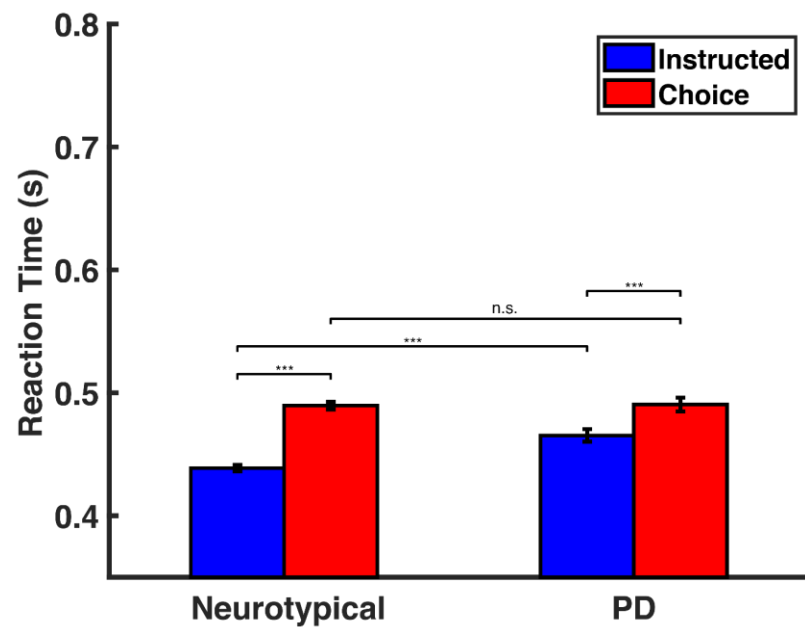
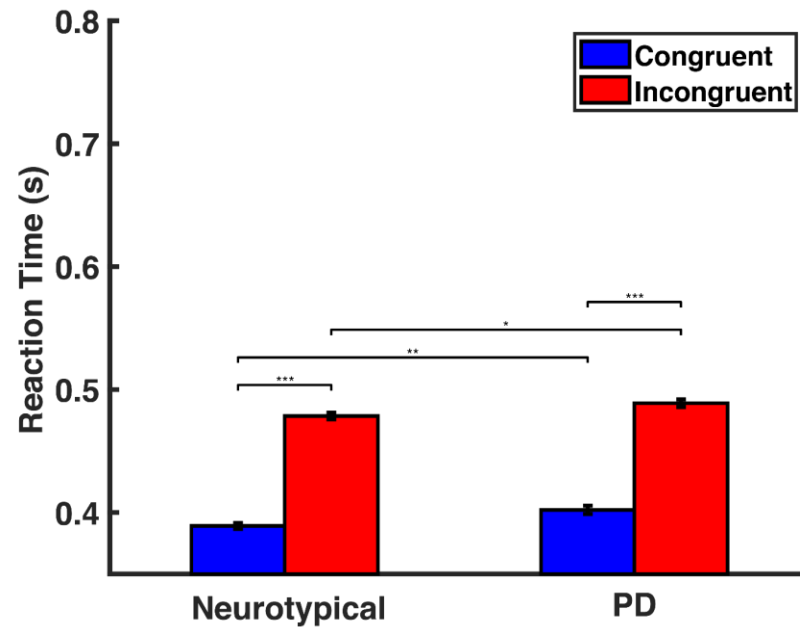
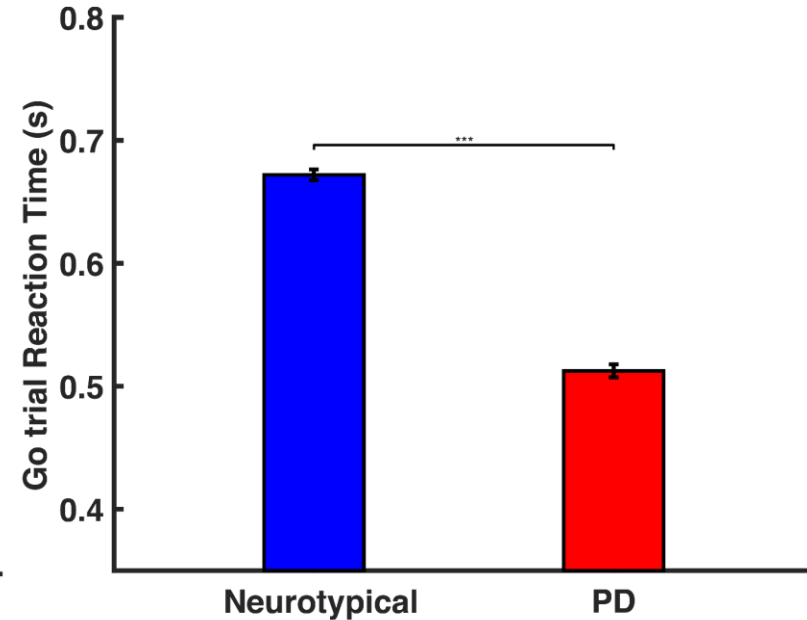


Figure 1

A**B****C****Figure 2**

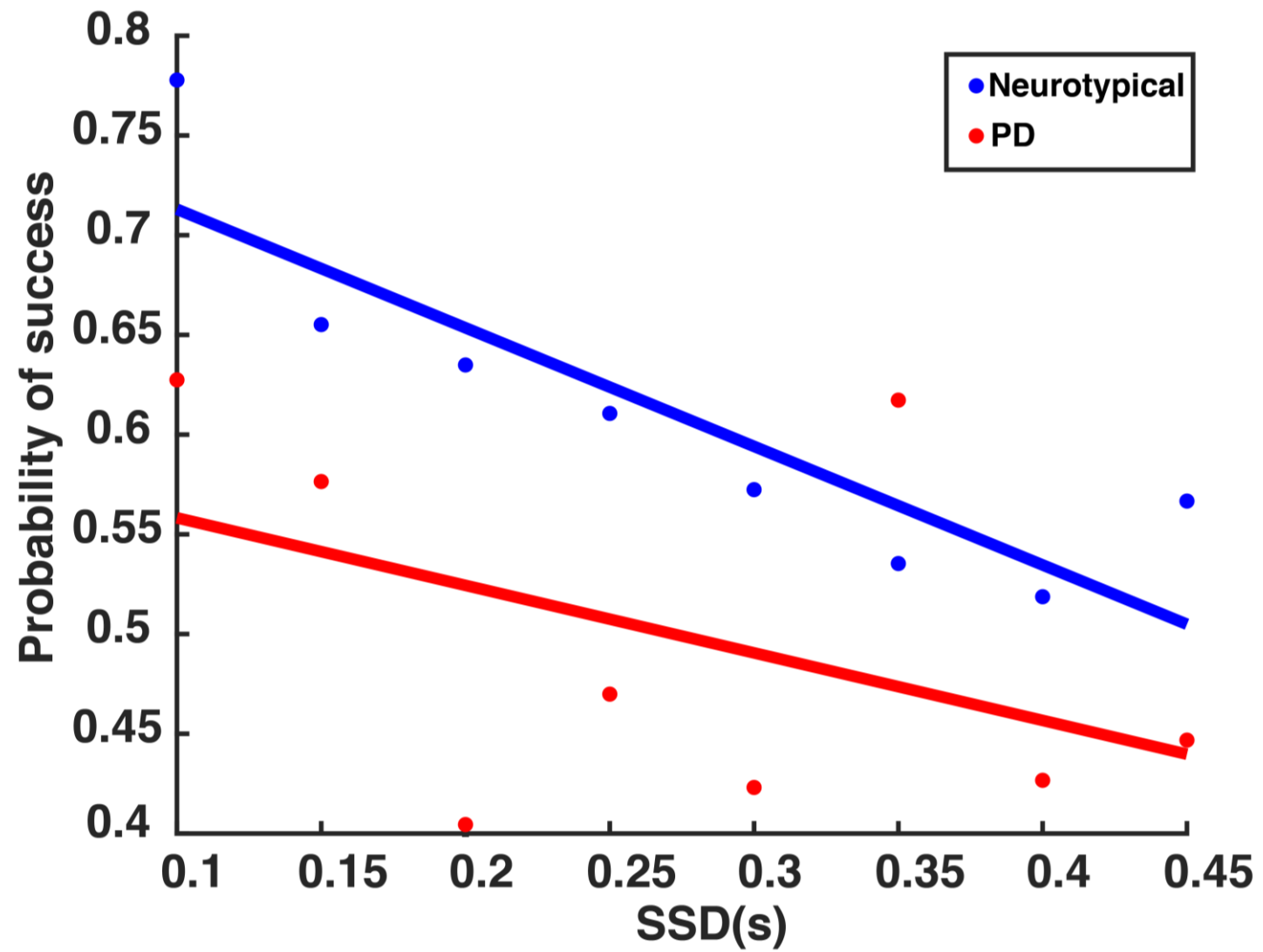


Figure 3

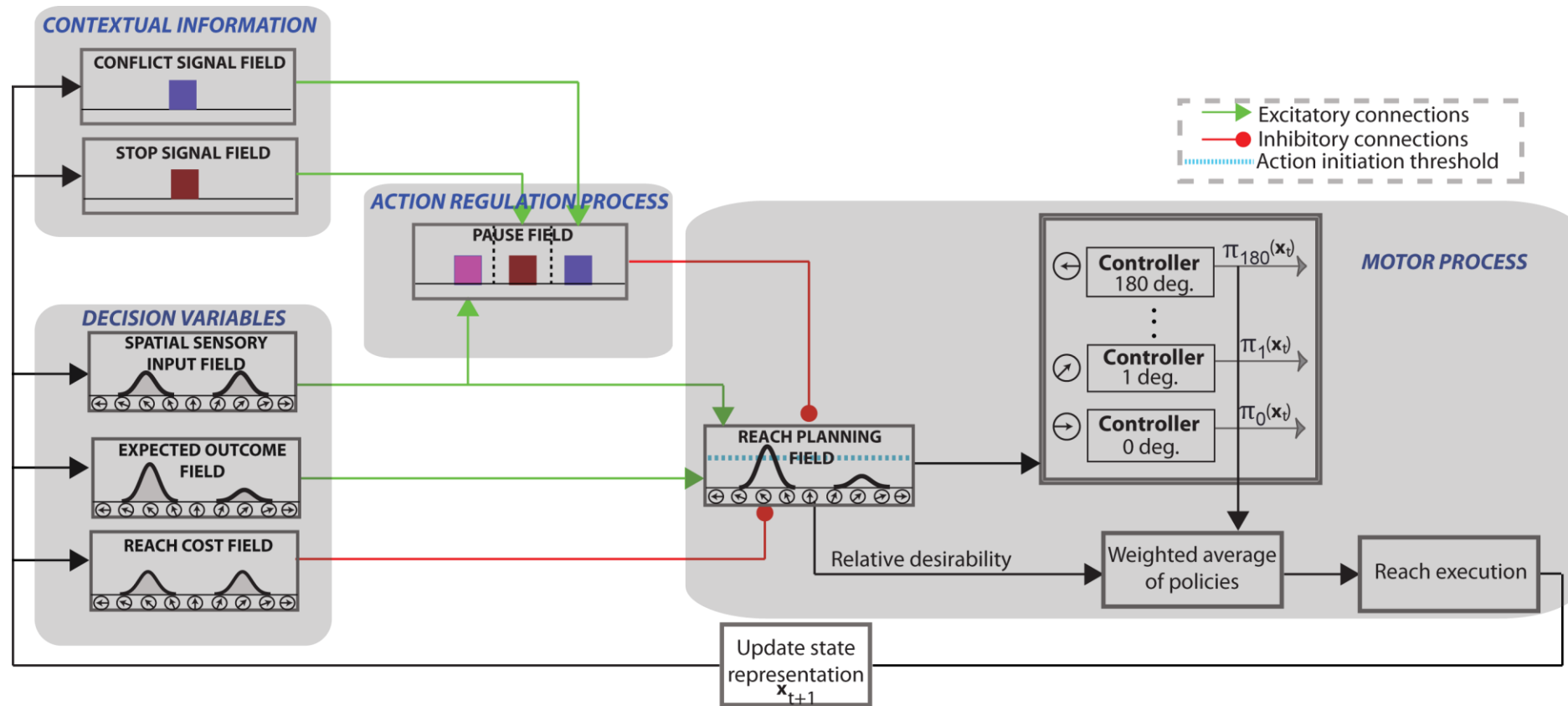


Figure 4

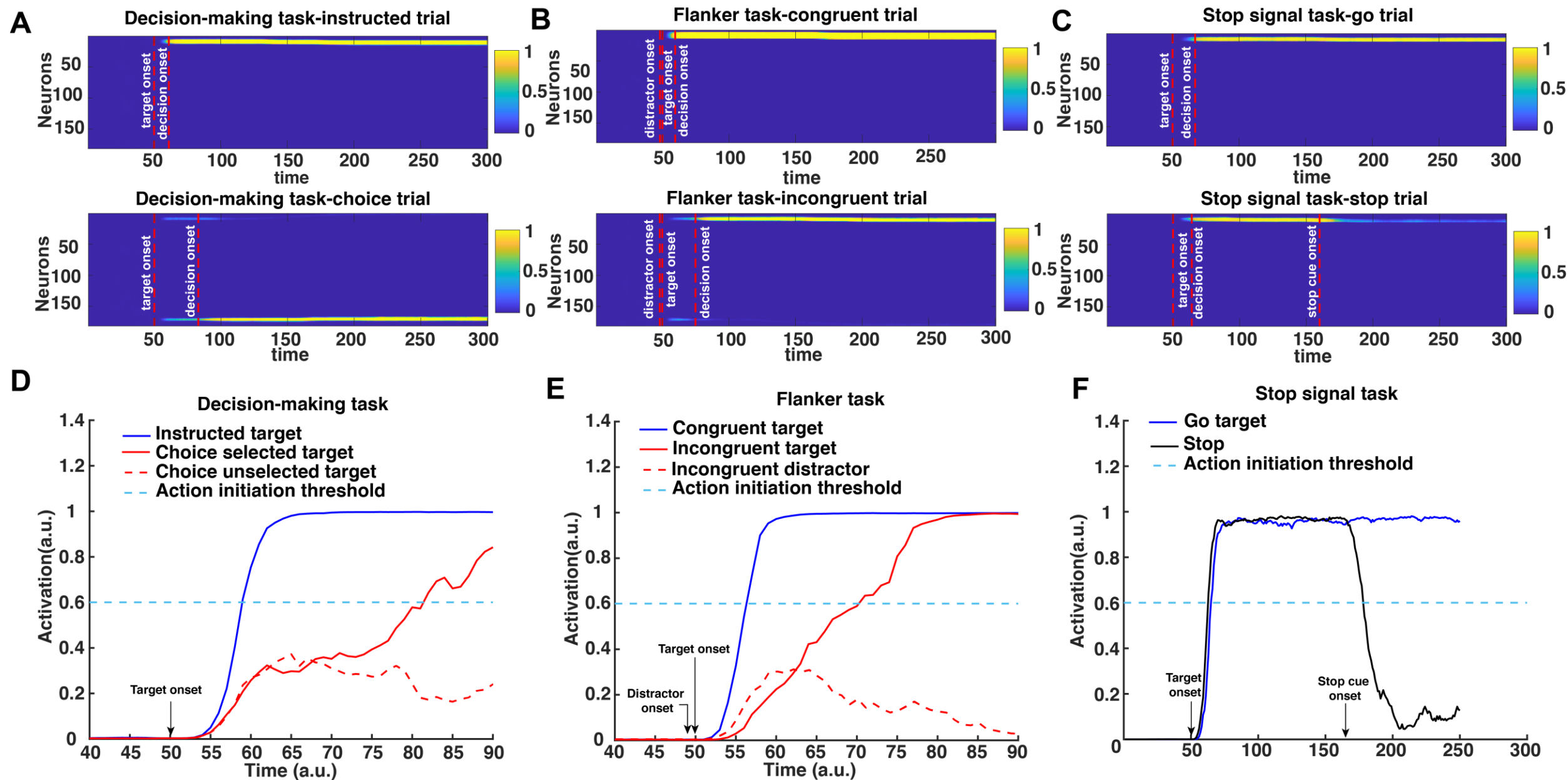


Figure 5

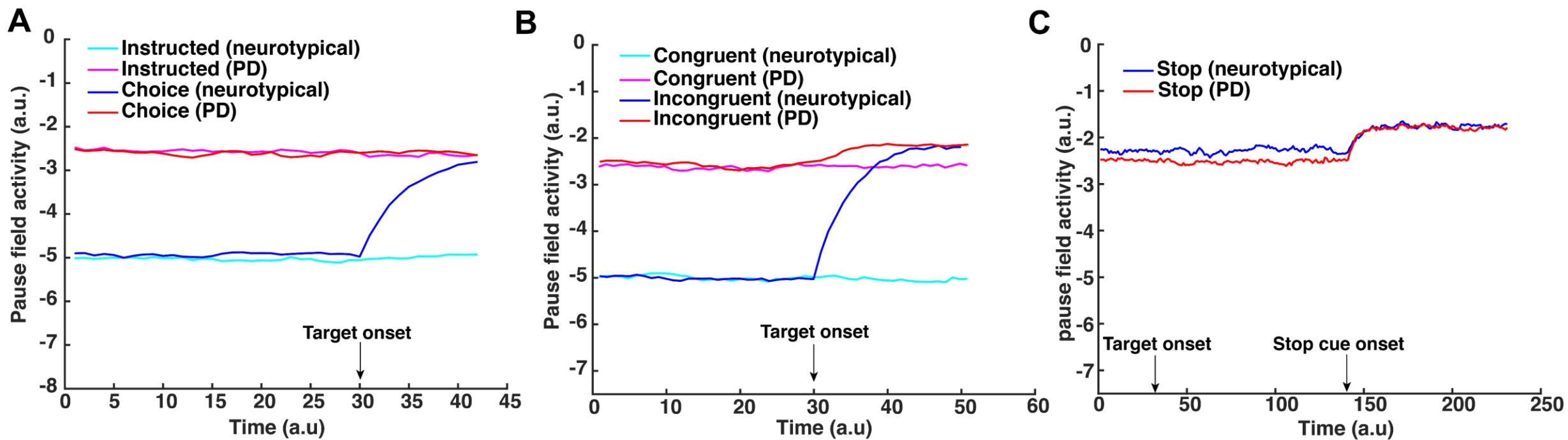


Figure 6

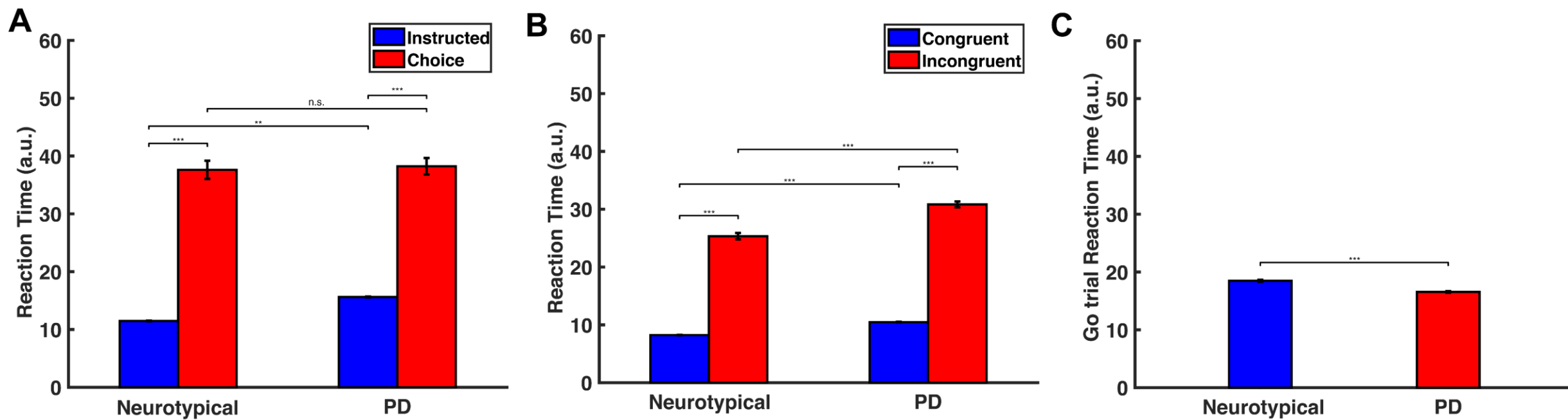


Figure 7

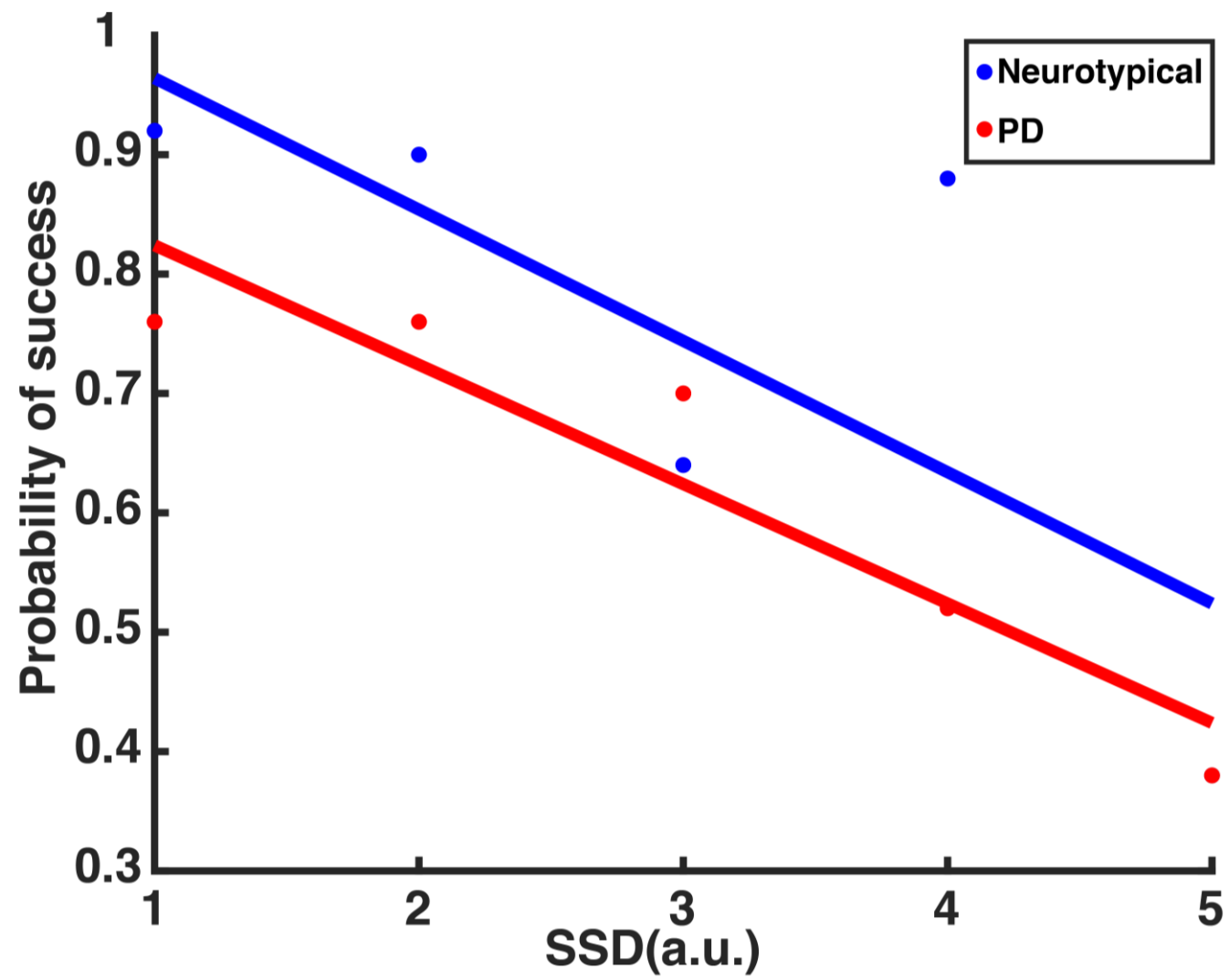


Figure 8

S1 Table

Model Parameters		
Parameters	Description	Value
η_{loc}	Visual input gain	8.5
η_{reward}	Expected outcome input gain	2.5
η_{cost}	Action cost input gain	-0.1
η_{pau}	Pause input gain	-4.0
γ	Action initiation threshold	0.6

Spatial sensory input field & Expected outcome field parameters		
Parameters	Description	Value
τ	Time constant	5.0
c_{exc}	Amplitude of excitatory portion of weight kernel	0
c_{inh}	Amplitude of inhibitory portion of weight kernel	0
σ_{exc}	Width of excitatory portion of weight kernel	5.0
σ_{inh}	Width of inhibitory portion of weight kernel	40.0
h	Resting activity level	-5.0
q	Noise level	0.25
σ_q	Width of noise kernel	5.0
β	Steepness of sigmoid activity function	1.0

Reach planning field parameters		
Parameters	Description	Value
τ	Time constant	5.0
c_{exc}	Amplitude of excitatory portion of weight kernel	0
c_{inh}	Amplitude of inhibitory portion of weight kernel	20
σ_{exc}	Width of excitatory portion of weight kernel	5.0
σ_{inh}	Width of inhibitory portion of weight kernel	180
h	Resting activity level	-5.0
q	Noise level	0.5
σ_q	Width of noise kernel	5.0
β	Steepness of sigmoid activity function	1.0

Pause field parameters		
Parameters	Description	Value
τ	Time constant	5.0
c_{exc}	Amplitude of excitatory portion of weight kernel	0
c_{inh}	Amplitude of inhibitory portion of weight kernel	0
σ_{exc}	Width of excitatory portion of weight kernel	5.0
σ_{inh}	Width of inhibitory portion of weight kernel	25.0
h	Resting activity level	-5.0
q	Noise level	0.25
σ_q	Width of noise kernel	5.0
β	Steepness of sigmoid activity function	1.0